Title
Enzymatic hydrolysis of ionic liquid-pretreated lignocellulose

Permalink
https://escholarship.org/uc/item/5b073871

Author
Shill, Kierston Ellen

Publication Date
2013

Enzymatic hydrolysis of ionic liquid - pretreated lignocellulose

by

Kierston Ellen Shill

A dissertation submitted in partial satisfaction of the

requirements for the degree of

Doctor of Philosophy

in

Chemical Engineering

in the

Graduate Division

of the

University of California, Berkeley

Committee in charge:

Professor Harvey W. Blanch, Co-Chair

Professor Douglas S. Clark, Co-Chair

Professor Chris R. Somerville

Fall 2013

Abstract

Enzymatic hydrolysis of ionic liquid - pretreated lignocellulose

by

Kierston Ellen Shill

Doctor of Philosophy in Chemical Engineering

University of California, Berkeley

Professors Douglas S. Clark and Harvey W. Blanch, Chairs

Cellulose is the most abundant organic compound on Earth, and is found in lignocellulosic biomass. In order to access this carbon source for biofuel production, a process must be developed that breaks down the natural barriers the plant has in place to protect itself from degradation. The natural breakdown of biomass by organisms involves a variety of enzymes that work together to make the carbon source available. Cellulose can be hydrolyzed in an acid-catalyzed process by cellulase enzymes to form glucose.

The enzymatic hydrolysis of cellulose relies on the initial adsorption of cellulases to the solid lignocellulose surface, and thus the reaction can be limited by surface area. Additionally, hemicellulose and lignin combine to act as barriers to adsorption, both physically and through competitive binding that inactivates the enzymes. Cellulose crystallinity also inhibits enzymatic degradation by limiting surface area and decreasing the rate of enzymatic hydrolysis. All of these factors make enzymatic hydrolysis of cellulose slow for untreated biomass, and make pretreatment a necessary step for biofuel production. Several pretreatment methods have been developed to make biomass more amenable to enzymatic hydrolysis. A promising approach is biomass dissolution in ionic liquids (ILs) followed by the addition of an anti-solvent to precipitate the cellulosic fraction of the biomass prior to hydrolysis. A cellulase mixture can then quickly and efficiently hydrolyze the precipitated biomass.

The enzymatic hydrolysis by a cellulase cocktail of *Miscanthus x giganteus*, a lignocellulosic biomass, pretreated with the IL 1-ethyl,3-methylimidazolium acetate ([Emim][OAc]) was studied. The IL pretreatment time and temperature parameters have been studied, and a kinetic model was developed to optimize the pretreatment conditions for improved cellulose and hemicellulose enzymatic conversion. This kinetic model indicated a wide range of optimal pretreatment conditions, from high temperatures / short times to lower temperatures / long times. Variables obtained from the kinetic model are within reported ranges of experimentally obtained values for other pretreatments, indicating that the model may be broadly applicable to a variety of lignocellulosic pretreatment processes.

Since ionic liquid pretreatment provides a readily-hydrolysable substrate, other factors, such as enzyme loading, product inhibition, and solids loading, become important. For industrially-relevant processes, the enzymatic hydrolysis must produce and tolerate high levels of glucose. We have investigated the effects of glucose concentration on the enzymatic hydrolysis of Avicel, [Emim][OAc]-pretreated Avicel, and [Emim][OAc]-pretreated *Miscanthus*. Both cellobiose and glucose production were monitored over time, and cellobiose was found to be present at appreciable concentrations when high levels of glucose were present. This effect is more pronounced with [Emim][OAc]-pretreated substrates. A competitive inhibition model was fit to the hydrolysis data and found to fit moderately well. However, this model was unable to capture both the fast initial glucose production and prolonged cellobiose presence, highlighting the need for a more mechanistic kinetic model.

By studying the enzymatic hydrolysis of pretreated lignocellulose, we will be able to better understand and direct the engineering of substrates, enzymes, and processes for more effective hydrolysis under industrially relevant conditions.

To my sister, for always listening, understanding, and telling me I’m not crazy.

Table of Contents

Chapter 1: An introduction to biofuels - pretreatment and enzymatic hydrolysis

Chapter 2: A model for optimizing the enzymatic hydrolysis of ionic liquid - pretreated lignocellulose

Chapter 3: Glucose inhibition of cellulase enzymes following ionic liquid pretreatment of lignocellulosic biomass

Acknowledgments

I would first like to thank my advisors Doug Clark and Harvey Blanch. They have given me a great amount of freedom to investigate what I found interesting, yet have provided guidance and support when I needed it. I would also like to thank Professor Chris Somerville for his helpful feedback and comments.

I would like to acknowledge the Clark lab for so many helpful discussions and advice, whether about work or life. They are the smartest group of people I know, and have pushed my knowledge and presentation skills to be the very best. I would specifically like to thank the Salad Club, Kathryn Strobel and Meera Atreya, who have literally fed me through this dissertation. I would also like to thank Katie Pfeiffer, Sarah Huffer Liszka, Annie Soler, and my entire ChE graduate class, who have constantly been there for me during my time in grad school.

I am grateful to Mara Bryan, Crystal Chan, and Stefan Bauer at the Energy Biosciences Institute for their help with lab equipment, supplies, and analysis. I would also like to thank Rocio Sanchez for helping me with my administrative needs. I would like to recognize the Energy Biosciences Institute for financial support for this project.

I would like to thank my family, especially Dad and Megan, for constantly believing in me and being only a phone call away. My pets, Gryphy, Tahina, and Cholula, have helped me immensely with their understanding and happy attitudes. Lastly, probably the single most important person for getting me through this has been Forrest, who has always been there for me, whether I needed a joke, shoulder to cry on, scientific advice, or delicious meal.

Curriculum Vitae

Education

University of California, Berkeley 2008 - 2013
(expected)

Ph.D. Chemical Engineering *(GPA: 3.88, minor: green chemistry)*
M.S. Chemical Engineering 2008 - 2010

Georgia Institute of Technology 2005 - 2008
B.S. Chemical and Biomolecular Engineering *(GPA: 3.88, with highest honor)*

Research Projects

University of California, Berkeley, Dissertation research 2008 - present
The pretreatment of lignocellulose with ionic liquids for improved enzymatic hydrolysis
PI: Douglas S. Clark and Harvey W. Blanch

Investigation and modeling of enzyme inhibition kinetics for biofuel production[5]

- Designed experiments to measure the impact of product inhibition on the enzymatic conversion of biomass to glucose
- Developed a kinetic model in Excel to explain and predict the product profiles obtained in experiments to compare with literature values
- Presented this work in a talk at an international conference

Optimization and modeling of ionic liquid pretreatment[1]

- Designed experiments to understand the pretreatment of biomass with ionic liquids
- Developed a model in MATLAB that characterized, predicted, and optimized the enzymatic hydrolysis of ionic liquid pretreated biomass
- Lead the publication of this work in a peer reviewed journal

Development and characterization of a novel ionic liquid recycle process[2,3]

- Worked in a team to develop an ionic liquid phase separation recycle process
- Performed lab scale experiments to integrate the recycle process into a pretreatment and enzymatic hydrolysis scheme
- Lead the publication of this work in a peer reviewed journal

University of California, Berkeley, Extracurricular research 2011 - present
Understanding marine oil spills: Improving decision making and identifying research needs[4]
PI: Martin J. Mulvihill

- Worked in an interdisciplinary team to develop a strategy for responding to oil spills in a marine environment
- Reviewed oil spill responses and their impacts on the environment

- Contributed equally with three other scientists on a publication submitted to a peer reviewed journal

Georgia Institute of Technology, Undergraduate research 2007 - 2008
Supercritical carbon dioxide as a novel solvent for separations
PI: Charles A. Eckert

- Built a supercritical fluid chromatograph for the separation of amino acids
- Designed and tested an FTIR high pressure cell
- Analyzed the tunability of separations for organic aqueous solvent systems

---

Publications

1. Shill, K., Miller, K., Clark, D.S., and Blanch, H.W. (2012) A model for optimizing the enzymatic hydrolysis of ionic liquid-pretreated lignocellulose. *Bioresource Technol.*, 126, p. 280-297.
2. **Shill, K.**, Padmanabhan, S., Xin, Q., Prausnitz, J.M., Clark, D.S., and Blanch, H.W. (2011) Ionic liquid pretreatment of cellulosic biomass: Enzymatic hydrolysis and ionic liquid recycle. *Biotechnol. Bioeng.*, 108 (3), p. 511-530.
3. **Shill, K.**, (2010) *The Application of Ionic Liquids to Improve the Enzymatic Hydrolysis of Lignocellulose.* Master's Thesis, University of California, Berkeley.
4. Andrade, K.*, Buckley, H.L.*, Rubin, L.K.*, **Shill, K.***, Mulvihill, M.J. (2013) Understanding marine oil spills: Improving decision making and identifying research needs. *Mar. Pollut. Bull.*, [Submitted]. *All authors contributed equally
5. **Shill, K.**, Clark, D.S., and Blanch, H.W. (2013) Glucose inhibition of cellulase enzymes following ionic liquid pretreatment of lignocellulosic biomass. [In preparation].

Presentations

Conferences:

Shill, K., Clark, D.S., and Blanch, H.W., An investigation of cellulase kinetics for efficient lignocellulose hydrolysis. 35th Symposium on Biotechnology for Fuels and Chemicals, Portland, OR., May 1, 2013.

Shill, K., Clark, D.S., and Blanch, H.W., Improved enzymatic hydrolysis of lignocellulose with ionic liquid pretreatment. 34th Symposium on Biotechnology for Fuels and Chemicals, New Orleans, LA., April 30, 2012.

Shill, K., Clark, D.S., and Blanch, H.W., The application of ionic liquids to improve enzymatic hydrolysis on lignocellulose. 33rd Symposium on Biotechnology for Fuels and Chemicals. Seattle, WA., May 3, 2011.

Other academic presentations:

Enzymatic hydrolysis of ionic liquid-pretreated lignocellulose., Energy Biosciences Institute Joint Lab Meeting., Berkeley, CA., August 15, 2013.

Enzymatic hydrolysis of ionic liquid-pretreated lignocellulose., Chemical and Biomolecular Engineering Department Colloquium, Berkeley, CA., April 17, 2013.

Enzymatic hydrolysis of ionic liquid pretreated lignocellulose., Energy Biosciences Institute Joint Lab Meeting., Berkeley, CA., August 5, 2010.

Technical skills

- Process development – developed and performed lab scale pretreatment, hydrolysis, and recycle processes for biofuels applications
- Kinetic and thermodynamic modeling – developed and applied fundamental models to novel systems using Microsoft Excel and MATLAB
- Enzymatic activity assays - developed and performed assays to detect the products of enzymatic hydrolysis with colorimetric assays, HPLC, UV-Vis, and the YSI Biochemistry Analyzer
- Protein quantification and purification – colorimetric assays, FPLC, LC-MS
- Designed, tested, and built high pressure systems for separations, UV-Vis, and FTIR
- Experience with COMSOL, Pymol, HTML, Aspen HYSYS

Leadership and Mentorship

University of California, Berkeley, Graduate Student Researcher 2011 - 2013

- Taught, supervised, and directed the research of two undergraduate student researchers in a laboratory environment, resulting in publication quality data

University of California, Berkeley, Graduate Student Instructor 2010 and 2012

Unit operations laboratory (2012)

- Instructed and supervised undergraduate students in a laboratory setting
- Lead office hours and graded presentations

Transport and separation processes (2010)

- Lead and organized discussion sections and office hours with undergraduate students
- Earned the student nominated Outstanding Teaching Award

The SMART Program, Volunteer tutor 2012 - present

- Tutored and mentored a student in middle school
- Helped supervise class field trip

Chapter 1

An introduction to biofuels - pretreatment and enzymatic hydrolysis

1. The role of biofuels

Our world is facing a crisis. For over a century, we have been relying on oil as a primary energy source for transportation and power, in addition to a starting material for many high volume commodity chemicals and products. However, easily accessible oil is running out. To combat this we have been drilling deeper, in the ocean, and in more sensitive environments, which is placing a burden on our planet and increasing the odds of environmentally catastrophic oil spills. While wind, solar, and nuclear energy are extremely promising technologies, there is a need for liquid transportation fuels that can readily be adapted to our current transportation requirements (Himmel et al., 2007; Huber et al., 2006). This new source of fuel needs to be renewable and less harmful to the environment.

Biofuels are the production of fuels from living organisms, such as plants. Using plant sources is a novel way to create a renewable fuel source by using carbon from our atmosphere and energy from the sun. Because of this process, using biofuels creates an efficient way of capturing solar energy, in addition to being a useful sink for carbon dioxide. The hope is that biofuels can be a transition away from fossil fuels to more diversified and renewable energy sources, with the added benefit of cleaning up our atmosphere and reducing net carbon emissions (Huber et al., 2006). However, biofuels require large amounts of land, water, and processing. Furthermore, plants used primarily for food are not a practical source since we do not want the demand for fuel to drive up the prices and availability of food. While the use of food sources for fuel, such as corn to ethanol, has been very important in understanding biofuel processing and drop-in fuel limitations, it is not a practical fuel source. Therefore, the use of non-food sources called lignocellulose, such as trees and grasses, should be the source for biofuel production (Somerville et al., 2010).

2. What is lignocellulose?

Lignocellulose is primarily composed of cellulose, hemicellulose, and lignin (Béguin and Aubert, 1994). It is found in the plant cell wall, and is what gives all plants their structure. Cellulose is a highly stable polymer made up of glucan chains comprised of repeating cellobiose units, or glucose dimers, linked together with β-O-4 bonds (See Figure 1), and makes up 20% to 60% of plants (Béguin and Aubert, 1994). Lignocellulosic biomass is converted to biofuels through hydrolysis of the polysaccharides into monomeric sugars, which can then be converted through fermentation into fuel (Himmel et al., 2007).

Hemicellulose is also a sugar polymer, but can be made up of several sugars, including glucose, xylose, and mannose. Unlike cellulose, hemicellulose is branched and non-crystalline (Béguin and Aubert, 1994). Lignin is covalently bound to hemicellulose through ester linkages. Lignin is an aromatic polymer composed of three main monomeric units, p-hydroxyphenyl, guaicyl, and syringyl, variously methoxylated and functionalized to bind together (Chundawat et al., 2011). These, combined with cellulose, give the plant its structural integrity and sugar storage.

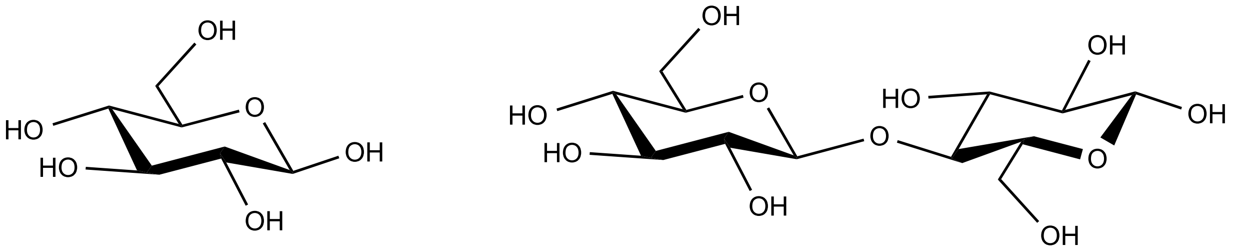

Figure 1. The chemical structures of glucose (monomer) and cellobiose (dimer), the components of cellulose.

The cellulose and hemicellulose may seem like a target for other organisms to attack and consume, but the structure of these are recalcitrant in nature. The cellulose, which is enticing because of its repeating glucose units, is actually very difficult for organisms to degrade. Glucan chains longer than six units are insoluble in physiological conditions, and can be up to 15,000 glucose units in length in the cell wall (Huber et al., 2006). Microfibrils are bundles of parallel glucan chains, bound together through an extensive network of hydrogen bonds between and within chains (See Figure 2). This highly crystalline network minimizes the amount of accessible surface area and chains available to attacking organisms, and the hydrogen bonding makes it difficult to remove a chain from the microfibril (Hall et al., 2010; Zhang and Lynd, 2004).

In addition to the cellulose itself being very difficult to access, the hemicellulose and lignin play parts in protecting the plant from degradation (Chernoglazov et al., 1988; Kumar et al., 2009). Hemicellulose, while not as difficult to degrade as cellulose because of its shorter chains (500-3000 sugar units) and branched, non-crystalline structure, can form physical barriers to the degradation of cellulose (Samayam and Schall, 2010). Lignin is a complex, cross-linked, aromatic polymer network that is extremely difficult to break up and disrupt. Generally, extreme conditions or free-radical chemistry is needed to break the bonds within lignin, which can then still reform to maintain its polymeric nature. These properties make it a strong physical barrier to organisms wishing to access the tempting sugars in the glucan chains. Additionally, because of lignin's hydrophobic aromatic structure, proteins sent to degrade glucans can instead bind and denatured on lignin (Berlin et al., 2005; Chernoglazov et al., 1988). Place all of this in the macrostructure of the plant cell wall, and the plant is quite well protected against many organisms wishing to partake of its sugar stores (Himmel et al., 2007).

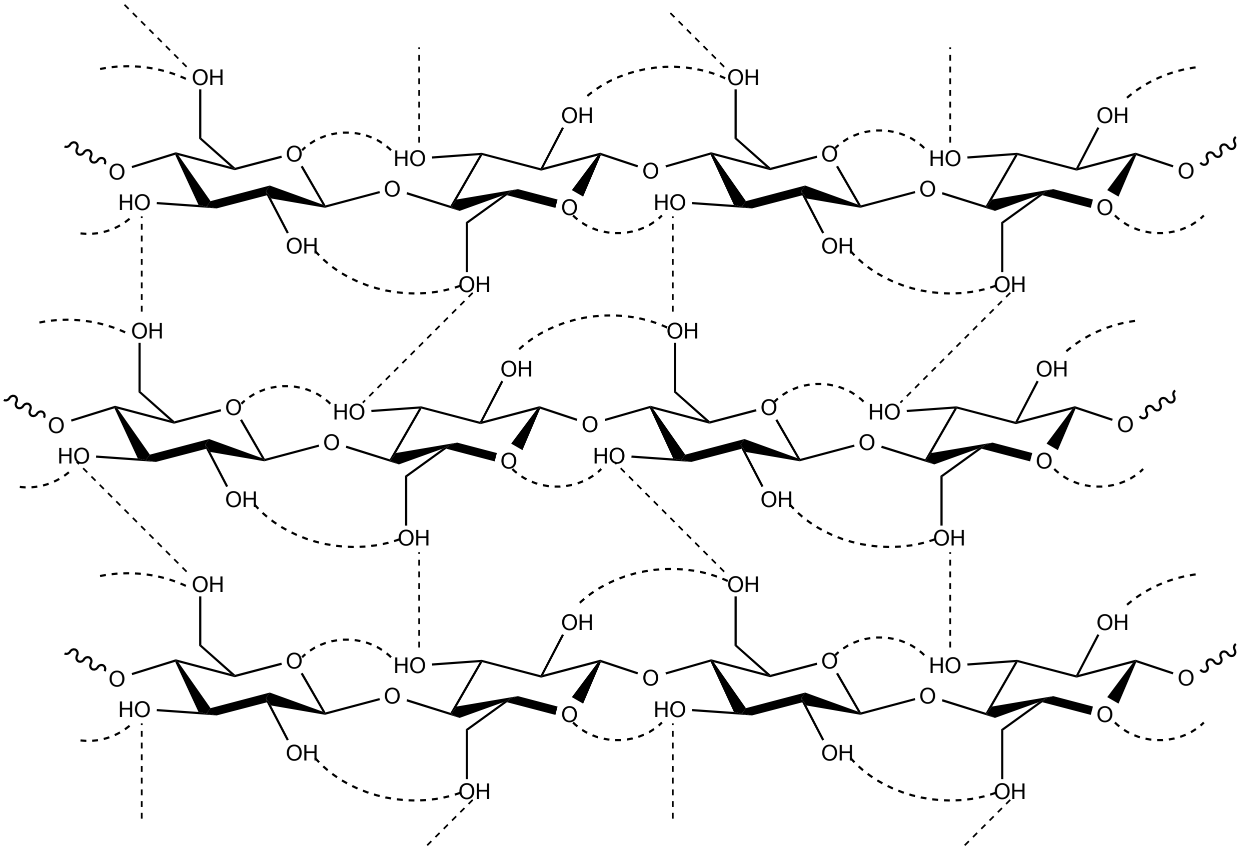

Figure 2. The structure of cellulose (Iβ, the crystalline structure most commonly found in plants). The dashed lines represent the hydrogen bonding within and between glucan chains.

3. How do organisms break down lignocellulose?

Certain organisms, however, have found very creative ways to access the glucans in spite of the plant's best efforts to dissuade them. The ability to hydrolyze cellulose to monomeric sugars has been achieved by organisms in every kingdom of life. These organisms produce enzymes, called cellulases, which have amino acid residues in their catalytic site that help react the glycosidic bonds with water (Kirby, 2001; Mosier et al., 2002; Reese et al., 1950; Sinnott, 1990). Likewise, there are a number of hemicellulases that hydrolyze hemicellulose. The enzymatic hydrolysis reactions are specific and yield only glucose monomers and oligomers, whereas mineral acid catalysts can further react with sugars to produce undesirable byproducts (Dee and Bell, 2011).

There are three main cellulases that are used to hydrolyze cellulose, endoglucanases, exoglucanases, and β-glucosidases. Endoglucanases bind to cellulose anywhere along the chain and hydrolyze. Exoglucanases must first find and bind to a chain end, and then can consecutively hydrolyze bonds along the glucan chain (Fox et al., 2012). Exoglucanases can work from both the reducing and non-reducing ends, and are believed to work progressively with a tunnel-like catalytic site that hydrolyzes the cellulose chain (Béguin and Aubert, 1994; Zhang et al., 2006). Endo and exoglucanases have two amino acid residues in their active site, either glutamic or aspartic acid, that catalyze the hydrolysis of the glycosidic bond. These residues are positioned on either side of the bond to be cleaved. Catalysis occurs when the pH of the reaction is near the pK_a of these amino acids, allowing one residue to exist protonated and the other deprotonated. The reaction then proceeds with one residue acting as a proton donor and the other as a base or nucleophile to facilitate the reaction of water with the glycosidic bond (Kirby, 2001; Mosier et al., 2002). These enzymes primarily produce cellobiose as their product, which is then hydrolyzed to glucose by the enzyme β-glucosidase (Reese et al., 1950). Some cellulases have binding domains attached to the catalytic domain, which help in binding to the cellulose (Béguin and Aubert, 1994). While the enzymes individually are ineffective at completely hydrolyzing cellulose, the full enzyme cocktail can work synergistically to reach appreciable hydrolysis and glucose production. Figure 3 shows a simplified scheme for the action of these enzymes on cellulose.

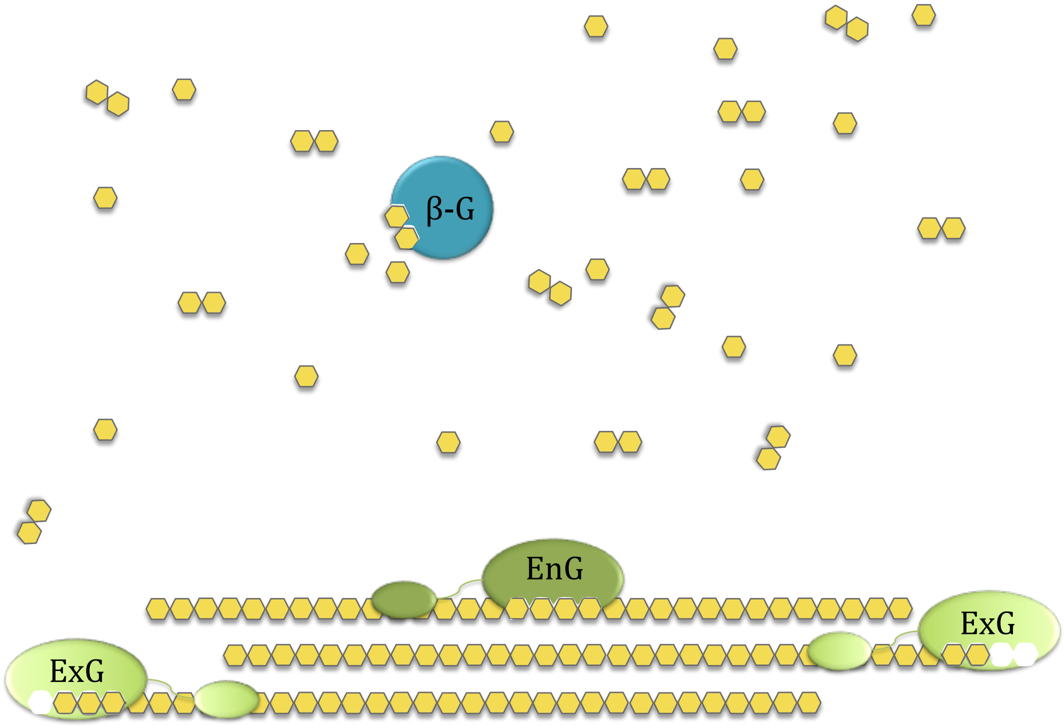

Figure 3. Simplified scheme for the enzymatic hydrolysis of insoluble cellulose by endoglucanases (EnG) and exoglucanases (ExG) to the soluble product cellobiose, which is then hydrolyzed by β-glucosidase (β-G) to glucose (Zhang et al., 2006).

One particular organism that is extremely effective at hydrolyzing crystalline cellulose is the fungus *Trichoderma reesei*. *T. reesei* was first discovered for its cellulose-degrading power during WWII because it was degrading cotton tents and clothing (Reese, 1976). Since then, it has been extensively studied and its enzymes well characterized for cellulose hydrolysis. It produces an enzymatic cocktail that can fully convert crystalline cellulose to glucose. It has multiple endoglucanases and two exoglucanases, in addition to two β-glucosidases (Heikinheimo, 2002). This cocktail is often supplemented with additional β-glucosidase from *Aspergillus niger*, which has been shown to help the overall conversion of lignocellulose by converting the cellobiose to glucose (Kadam et al., 2004; Sternberg et al., 1977).

4. What is pretreatment?

However, even this highly developed system does not meet the needs of biofuel production. For a cost-effective biofuels process, hydrolysis needs to be performed at a high solid to liquid ratio, with minimal protein usage, and should reach very high glucose concentrations in as short a time as possible. Organisms have not necessarily evolved in nature for these conditions. Therefore, there is much engineering and process development to be done in order to make enzymatic hydrolysis a viable biofuels process.

Because of the plant's recalcitrant nature, enzymes are often very slow to convert the glucans to sugars. Enzymatic catalysis relies on the initial adsorption of enzymes to the solid lignocellulose surface, and thus the reaction can be limited by surface area. Additionally, hemicellulose and lignin combine to act as a barrier to adsorption, both physically and through competitive binding that inactivates the enzymes (Berlin et al., 2005). Cellulose crystallinity also inhibits enzymatic degradation by limiting surface area and decreasing the rate of enzymatic hydrolysis (Himmel et al., 2007). All of these factors make enzymatic hydrolysis of cellulose slow for untreated biomass. One of the ways that these issues can be alleviated is to introduce a treatment before hydrolysis, called pretreatment.

Pretreatments can be chemical, mechanical, thermal, or biological, and have a wide range of effects on lignocellulose (See Table 1). The goal of pretreatment is to make the plant easier to hydrolyze, while preventing the loss of sugars. Therefore, a pretreatment must be effective enough to significantly improve enzymatic hydrolysis, but cannot be too harsh. A harsh pretreatment can result in the degradation of sugars to byproducts, similar to a caramelization process, which would decrease the overall efficiency and potentially harm downstream fermentation (Huffer et al., 2012). Ultimately, the hydrolysis benefits must out-way the cost of a pretreatment for it to be adopted in a biofuels process.

Process	Examples	Effects	Issues
Mechanical	Milling, steam, AFEX	Increases surface area	Energy cost
Thermal	Hot water	Increases surface area, removes hemicellulose	Byproduct formation
Chemical	Dilute sulfuric acid, concentrated acid, NaOH	Hydrolysis of bonds, hemicellulose and lignin modification/removal	Corrosive, byproduct formation
Biological	Enzymatic, Fungal	Degrades cell wall, delignification	Slow
Solvents	Ammonia, OrganoSolv, NMMO, ILs	Partial or full solubilization of the plant, decrystallization of cellulose	Recycle

Table 1. The different categories of pretreatment processes, with relevant examples, effects on lignocellulose, and issues for biofuels adoption (Deguchi et al., 2006; Huber et al., 2006; Kumar et al., 2009; Murnen et al., 2007; Sun and Cheng, 2002).

5. Ionic liquid pretreatment

Ionic liquid, or IL, pretreatment is a relatively new process to that has been applied to biofuel production (Kilpeläinen et al., 2007; Swatloski et al., 2002). The Rogers group discovered in 2002 that the ionic liquid 1-butyl,3-methylimidazolium chloride completely dissolved cellulose (Remsing et al., 2006; Swatloski et al., 2002). Since this discovery, a variety of ionic liquids have been tested on many different lignocellulosic substrates and biomass solvation in ILs has been found to provide a very effective pretreatment (Fukaya et al., 2008; Zhang et al., 2005; Zhu et al., 2006). The ionic liquid 1-ethyl,3-methylimidazolium acetate, or [Emim][OAc] (See Figure 4), is able to dissolve a variety of different whole lignocellulosic substrates (Sun et al., 2009; Zavrel et al., 2009), resulting in decrystallized material that is readily degraded by cellulases (Arora et al., 2010; Kilpeläinen et al., 2007; Lee et al., 2009; Samayam and Schall, 2010; Shill et al., 2011; Zhao et al., 2010).

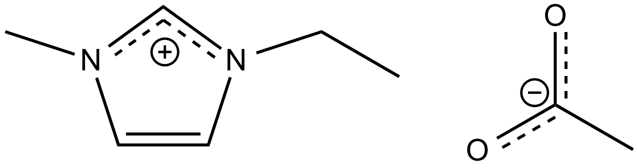

Figure 4. The chemical structure of the ionic liquid [Emim][OAc].

Ionic liquids are salts that are liquid at or near room temperature, composed of an organic cation and organic or inorganic anion (Zhao et al., 2009). [Emim][OAc] is thought to dissolve cellulose by intercalating into and breaking up the hydrogen-bonding network of the cellulose (Cheng et al., 2012; Gross and Chu, 2010; Remsing et al., 2006; Singh et al., 2009). [Emim][OAc] works particularly well at dissolving lignocellulose because of the aromatic nature of the cation, which allows it to interact through ring, or π-π, stacking with the lignin (Kilpeläinen et al., 2007; Lee et al., 2009). These interactions allow [Emim][OAc] to dissolve large amounts of cellulose (>10 wt%), lignin (~30 wt%), and lignocellulosic biomass of various types (~5 wt%), with minimal milling or drying (Lee et al., 2009; Shill et al., 2012; Shill et al., 2011; Sun et al., 2009; Zavrel et al., 2009).

The cellulose is readily precipitated by the addition of water, with partial hemicellulose and lignin precipitation (Shill et al., 2011). The resulting precipitate is decrystallized cellulose with increased surface area and partial lignin removal, and no overall plant wall structure remaining (Arora et al., 2010; Swatloski et al., 2002). Figure 5 shows 1 g of *Miscanthus*, a lignocellulosic energy grass, before and after IL pretreatment, and illustrates the physical changes that occur. The IL-pretreated biomass can be easily washed with additional water to remove any excess IL present, and readily hydrolyzed by a *T. reesei* cellulase cocktail to its monomeric sugars (Shill et al., 2012; Shill et al., 2011). Figure 6 shows the simplified process diagram for IL pretreatment.

Figure 5. One gram of *Miscanthus* before and after IL pretreatment.

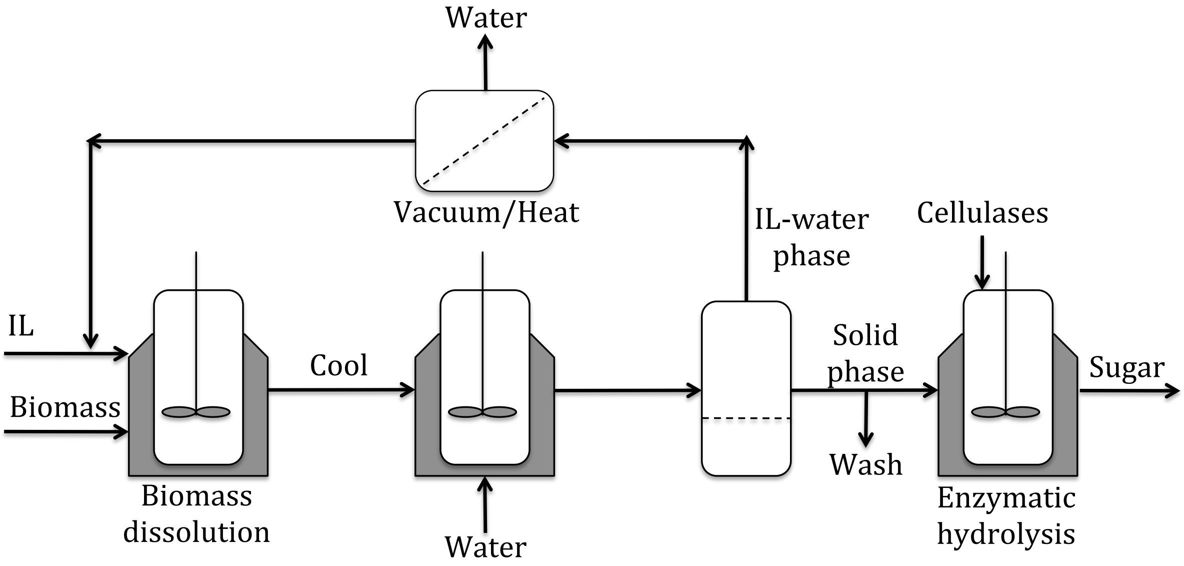

Figure 6. Simplified process diagram for the pretreatment of biomass with IL.

IL pretreatment is appealing from a processing point of view for many reasons. The IL can be recycled by evaporation of the water or phase separation (Binder and Raines, 2010; Shill et al., 2011; Varanasi et al., 2008). In addition, many ILs are considered green solvents and easily handled on a large scale because of their lack of vapor pressure, recyclability, and non-corrosive properties, reducing the need for specialized equipment or environmental release concerns (Binder and Raines, 2010; Li et al., 2010). IL pretreatment also has benefits for biofuels production other than its ability to drastically minimize hydrolysis time. Because they are solvents and do not generally react with biomass, ILs do not generally produce byproducts. This is beneficial because byproducts can reduce overall conversion and inhibit downstream fermentation (Binder and Raines, 2010; Huffer et al., 2012; Li et al., 2010; Li et al., 2009).

6. Economic barriers to IL pretreatment

However, the recyclability and solvent nature of ILs can also be their downside economically. Because of their relatively recent discovery and low demand, ILs are currently quite expensive and require recycling in order to be economic (Binder and Raines, 2010). In addition, the antisolvent needed to precipitate the biomass must be removed before the IL can be reused, which places a separation burden on the process. If water is used as the antisolvent, then large quantities of water must be evaporated, resulting in a significant energy cost (Binder and Raines, 2010; Varanasi et al., 2010). Furthermore, there is still some concern that some of the components from the biomass that do not precipitate, primarily lignin, could build up and decrease the efficiency of the pretreatment process (Shill et al., 2011; Xin et al., 2012).

Some progress has been made to allay these concerns. Kosmotropic salt solutions have been used to induce a phase separation between water and [Emim][OAc], resulting in partial removal of the water from the IL (Shill et al., 2011). Organic phase separations have been studied to help remove the biomass components from the IL phase (Dibble et al., 2011; Xin et al., 2012). Moreover, extensive economic and process modeling has been conducted, showing that simple process design, combined with a decrease in [Emim][OAc] costs due to economies of scale, can result in IL pretreatment being cost competitive with dilute acid pretreatment (Klein-Marcuschamer et al., 2011b). An increase in the solids to IL ratio, without full dissolution, decreases the amount of IL needed and still results in an enzymatically-hydrolyzable biomass (Cheng et al., 2012). Novel ILs have also been discovered that are much easier to make, from cheaper starting material compared to [Emim][OAc], and still able to pretreat lignocellulose (Liu et al., 2012).

7. Enzymatic hydrolysis issues

Because IL pretreatment has shown to greatly enhance the enzymatic hydrolysis of lignocellulose, aspects of the hydrolysis can be further studied and optimized. For biological fermentation processes to convert the sugar to fuel, a sugar stream > 100 g/L is needed from the enzymatic hydrolysis (Andrić et al., 2010). Assuming enzymatic hydrolysis reaches 100% conversion, this production target requires at least a 14 wt% lignocellulose solution during hydrolysis. Moreover, less than 20 mg of protein is required per gram of cellulose for the process to be economical because of the high cost of cellulase production (Klein-Marcuschamer et al., 2011a). The enzyme costs are also due to the cellulases' strong binding affinity for any remaining cellulose or lignin, causing the enzymes to be lost. Instead of being reusable catalysts, the cellulases become costly reactants. Temperature instability of cellulases can also cause them to be less efficient (Liszka et al., 2012).

In summary, for enzymatic hydrolysis to be economical, it not only needs to reach a high conversion in a short amount of reaction time, but to perform at high solids loadings, low cellulase loadings, and attaining high product concentrations. While IL pretreatment allows us to reach high conversions in small hydrolysis times with low concentrations of protein, this has mostly been studied at low solids loadings and obtaining glucose concentrations of only 10 g/L. High solids loadings can be an issue for many reasons, including viscosity and mixing challenges for process and equipment design, and loss of cellulases due to inactive binding (Gusakov et al., 1987). In addition, obtaining high concentrations of sugars can result in decreased enzymatic efficiency because the sugars inhibit the enzymes from further hydrolyzing fresh cellulose. As a result, the study and optimization of enzymatic hydrolysis at more realistic biofuel conditions is an active area of research. A thorough understanding in the mechanism of cellulase product inhibition on lignocellulosic substrates is needed for enzymes to be engineered for improved recyclability and decreased inhibition.

8. Outline of dissertation

Previous work addressed the issue of ionic liquid costs with a novel ionic liquid recycle process. In this study, we developed a system where water could be removed through the addition of kosmotropic salts (Shill et al., 2011). The work also laid the groundwork for IL pretreatment process methods in addition to enzymatic hydrolysis time course methods (Shill, 2010). This dissertation should be seen as a continuation and expansion of that work.

In Chapter 2, the optimization and investigation of IL pretreatment is discussed. The goal of this work was to investigate the best pretreatment conditions for enzymatic hydrolysis of lignocellulose. Since ILs are a relatively new form of pretreatment, an investigation of pretreatment temperature and time was needed to understand the thermodynamics and kinetics of the pretreatment process, and optimize it for the enzymatic hydrolysis of lignocellulose (Shill et al., 2012).

In Chapter 3, the enzymatic hydrolysis is studied further. Since IL-pretreated material is readily hydrolyzed by a cellulase cocktail, we strove to further optimize the hydrolysis process. After initial studies, we quickly found that product inhibition was a major contributing factor to the decreased conversion of lignocellulose at high solids loadings. This work focuses on the enzymatic hydrolysis of IL-pretreated material at varying initial glucose concentrations to understand the degree of inhibition and its effects on cellobiose and glucose production over time from a cellulase cocktail. In addition, we studied the process with a competitive inhibition kinetic model to further understand the parameters important in characterizing hydrolysis under inhibitory conditions.

References

Andrić, P., Meyer, A.S., Jensen, P.A., Dam-Johansen, K., 2010. Reactor design for minimizing product inhibition during enzymatic lignocellulose hydrolysis: I. Significance and mechanism of cellobiose and glucose inhibition on cellulolytic enzymes. Biotechnol. Adv. 28, 308-324.

Arora, R., Manisseri, C., Li, C., Ong, M.D., Scheller, H.V., Vogel, K., Simmons, B.A., Singh, S., 2010. Monitoring and Analyzing Process Streams Towards Understanding Ionic Liquid Pretreatment of Switchgrass (*Panicum virgatum* L.). Bioenerg. Res. 3, 134-145.

Béguin, P., Aubert, J.-P., 1994. The biological degradation of cellulose. FEMS Microbiol. Rev. 13, 25-58.

Berlin, A., Gilkes, N., Kurabi, A., Bura, R., Tu, M., Kilburn, D., Saddler, J., 2005. Weak lignin-binding enzymes: a novel approach to improve activity of cellulases for hydrolysis of lignocellulosics. Appl. Biochem. Biotechnol. 121-124, 163-170.

Binder, J.B., Raines, R.T., 2010. Fermentable sugars by chemical hydrolysis of biomass. Proc. Natl. Acad. Sci. U. S. A. 107, 4516-4521.

Cheng, G., Varanasi, P., Arora, R., Stavila, V., Simmons, B.A., Kent, M.S., Singh, S., 2012. Impact of Ionic Liquid Pretreatment Conditions on Cellulose Crystalline Structure Using 1-Ethyl-3-methylimidazolium Acetate. J. Phys. Chem. B 116, 10049-54.

Chernoglazov, V.M., Ermolova, O.V., Klyosov, A.A., 1988. Adsorption of high-purity endo-1,4-beta-glucanases from Trichoderma-reesei on components of lignocellulosic materials - cellulose, lignin, and xylan. Enzyme Microb. Technol. 10, 503-507.

Chundawat, S.P.S., Beckham, G.T., Himmel, M.E., Dale, B.E., 2011. Deconstruction of lignocellulosic biomass to fuels and chemicals. Annu. Rev. Chem. Biomol. Eng. 2, 6.1-6.25.

Dee, S., Bell, A.T., 2011. Effects of reaction conditions on the acid-catalyzed hydrolysis of miscanthus dissolved in an ionic liquid. Green Chem. 13, 1467-1475.

Deguchi, S., Tsujii, K., Horikoshi, K., 2006. Cooking cellulose in hot and compressed water. Chem. Commun., 3293-3295.

Dibble, D.C., Li, C., Sun, L., George, A., Cheng, A., Çetinkol, Ö., Benke, P., Holmes, B.M., Singh, S., Simmons, B.A., 2011. A facile method for the recovery of ionic liquid and lignin from biomass pretreatment. Green Chem. 13, 3255-3264.

Fox, J.M., Levine, S.E., Clark, D.S., Blanch, H.W., 2012. Initial- and Processive-Cut Products Reveal Cellobiohydrolase Rate Limitations and the Role of Companion Enzymes. Biochemistry 51, 442-452.

Fukaya, Y., Hayashi, K., Wada, M., Ohno, H., 2008. Cellulose dissolution with polar ionic liquids under mild conditions: required factors for anions. Green Chem. 10, 44-46.

Gross, A.S., Chu, J.-W., 2010. On the Molecular Origins of Biomass Recalcitrance: The Interaction Network and Solvation Structures of Cellulose Microfibrils. J. Phys. Chem. B 114, 13333-13341.

Gusakov, A.V., Sinitsyn, A.P., Klyosov, A.A., 1987. Factors Affecting the Enzymatic Hydrolysis of Cellulose in Batch and Continuous Reactors: Computer Simulation and Experiment. Biotechnol. Bioeng. XXIX, 906-910.

Hall, M., Bansal, P., Lee, J.H., Realff, M.J., Bommarius, A.S., 2010. Cellulose crystallinity- a key predictor of the enzymatic hydrolysis rate. FEBS J. 277, 1571-1582.

Heikinheimo, L. 2002. Trichoderma reesei cellulases in processing of cotton, VTT Publications, pp. 82.

Himmel, M.E., Ding, S.-Y., Johnson, D.K., Adney, W.S., Nimlos, M.R., Brady, J.W., Foust, T.D., 2007. Biomass Recalcitrance: Engineering Plants and Enzymes for Biofuels Production. Science 315, 804-807.

Huber, G.W., Iborra, S., Corma, A., 2006. Synthesis of Transportation Fuels from Biomass: Chemistry, Catalysts, and Engineering. Chem. Rev. 106, 4044-4098.

Huffer, S., Roche, C.M., Blanch, H.W., Clark, D.S., 2012. Escherichia coli for biofuel production: bridging the gap from promise to practice. Trends Biotechnol. 30, 538-545.

Kadam, K.L., Rydholm, E.C., McMillan, J.D., 2004. Development and validation of a kinetic model for enzymatic saccharification of lignocellulosic biomass. Biotechnol Prog 20, 698-705.

Kilpeläinen, I., Xie, H., King, A., Granstrom, M., Heikkinen, S., Argyropoulos, D.S., 2007. Dissolution of Wood in Ionic Liquids. J. Agric. Food Chem. 55, 9142-9148.

Kirby, A.J., 2001. The lysozyme mechanism sorted - after 50 years. Nat. Struct. Biol. 8, 737-739.

Klein-Marcuschamer, D., Oleskowicz-Popiel, P., Simmons, B.A., Blanch, H.W., 2011a. The challenge of enzyme cost in the production of lignocellulosic biofuels. Biotechnol. Bioeng. 109, 1083-1087.

Klein-Marcuschamer, D., Simmons, B.A., Blanch, H.W., 2011b. Techno-economic analysis of a lignocellulosic ethanol biorefinery with ionic liquid pre-treatment. Biofuels, Bioprod. Biorefin. 5, 562-569.

Kumar, P., Barrett, D.M., Delwiche, M.J., Stroeve, P., 2009. Methods for Pretreatment of Lignocellulosic Biomass for Efficient Hydrolysis and Biofuel Production. Ind. Eng. Chem. Res. 48, 3713-3729.

Lee, S.H., Doherty, T.V., Linhardt, R.J., Dordick, J.S., 2009. Ionic Liquid-Mediated Selective Extraction of Lignin From Wood Leading to Enhanced Enzymatic Cellulose Hydrolysis. Biotechnol. Bioeng. 102, 1368-1376.

Li, C.L., Knierim, B., Manisseri, C., Arora, R., Scheller, H.V., Auer, M., Vogel, K.P., Simmons, B.A., Singh, S., 2010. Comparison of dilute acid and ionic liquid pretreatment of switchgrass: Biomass recalcitrance, delignification and enzymatic saccharification. Bioresour. Technol. 101, 4900-4906.

Li, Q., He, Y.-C., Xian, M., Jun, G., Xu, X., Yang, J.-M., Li, L.-Z., 2009. Improving enzymatic hydrolysis of wheat straw using ionic liquid 1-ethyl-3-methyl imidazolium diethyl phosphate pretreatment. Bioresour. Technol. 100, 3570-3575.

Liszka, M.J., Clark, M.E., Schneider, E., Clark, D.S., 2012. Nature Versus Nurture: Developing Enzymes That Function Under Extreme Conditions. Annu. Rev. Chem. Biomol. Eng. 3, 77-102.

Liu, Q.-P., Hou, X.-D., Li, N., Zong, M.-H., 2012. Ionic liquids from renewable biomaterials: synthesis, characterization and application in the pretreatment of biomass. Green Chem. 14, 304-307.

Mosier, N.S., Ladisch, C.M., Ladisch, M.R., 2002. Characterization of acid catalytic domains for cellulose hydrolysis and glucose degradation. Biotechnol. Bioeng. 79, 610-618.

Murnen, H.K., Balan, V., Chundawat, S.P.S., Bals, B., Sousa, L.D., Dale, B.E., 2007. Optimization of ammonia fiber expansion (AFEX) pretreatment and enzymatic hydrolysis of Miscanthus x giganteus to fermentable sugars. Biotechnol. Prog. 23, 846-850.

Reese, E.T., 1976. History of the cellulase program at the U.S. army Natick Development Center. Biotechnol. Bioeng. Symp. 6, 9-20.

Reese, E.T., Siu, R.G.H., Levinson, H.S., 1950. The biological degradation of soluble cellulose derivatives and its relationship to the mechanism of cellulose hydrolysis. J. Bacteriol. 59, 485-497.

Remsing, R.C., Swatloski, R.P., Rogers, R.D., Moyna, G., 2006. Mechanism of cellulose dissolution in the ionic liquid 1-n-butyl-3-methylimidazolium chloride: a ^{13}C and $^{35/37}$Cl NMR relaxation study on model systems. Chem. Commun., 1271-1273.

Samayam, I.P., Schall, C.A., 2010. Saccharification of ionic liquid pretreated biomass with commercial enzyme mixtures. Bioresour. Technol. 101, 3561-3566.

Shill, K., Miller, K., Clark, D.S., Blanch, H.W., 2012. A model for optimizing the enzymatic hydrolysis of ionic liquid-pretreated lignocellulose. Bioresour. Technol. 126, 290-297.

Shill, K., Padmanabhan, S., Xin, Q., Prausnitz, J.M., Clark, D.S., Blanch, H.W., 2011. Ionic liquid pretreatment of cellulosic biomass: Enzymatic hydrolysis and ionic liquid recycle. Biotechnol. Bioeng. 108, 511-520.

Shill, K.E. 2010. The application of ionic liquids to improve the enzymatic hydrolysis of lignocellulose, MS thesis, University of California, Berkeley.

Singh, S., Simmons, B.A., Vogel, K.P., 2009. Visualization of Biomass Solubilization and Cellulose Regeneration During Ionic Liquid Pretreatment of Switchgrass. Biotechnol. Bioeng. 104, 68-75.

Sinnott, M.L., 1990. Catalytic Mechanisms of Enzymic Glycosyl Transfer. Chem. Rev. 90, 1171-1202.

Somerville, C., Youngs, H., Taylor, C., Davis, S.C., Long, S.P., 2010. Feedstocks for Lignocellulosic Biofuels. Science 329, 790-792.

Sternberg, D., Vijayakumar, P., Reese, E.T., 1977. β-Glucosidase: microbial production and effect on enzymatic hydrolysis of cellulose. Can. J. Microbiol. 23, 139-147.

Sun, N., Rahman, M., Qin, Y., Maxim, M.L., Rodríguez, H., Rogers, R.D., 2009. Complete dissolution and partial delignification of wood in the ionic liquid 1-ethyl-3-methylimidazolium acetate. Green Chem. 11, 646-655.

Sun, Y., Cheng, J., 2002. Hydrolysis of lignocellulosic materials for ethanol production: a review. Bioresour. Technol. 83, 1-11.

Swatloski, R.P., Spear, S.K., Holbrey, J.D., Rogers, R.D., 2002. Dissolution of Cellose with Ionic Liquids. J. Am. Chem. Soc. 124, 4974-4975.

Varanasi, S., Schall, C.A., Dadi, A.P. 2010. Saccharifying cellulose. US Patent 7674608 B2. The University of Toledo.

Varanasi, S., Schall, C.A., Dadi, A.P., Anderson, J., Rao, K., Paripati, P., Kumar, G. 2008. Biomass Pretreatment. US Patent 8030030 B2. The University of Toledo.

Xin, Q., Pfeiffer, K., Prausnitz, J.M., Clark, D.S., Blanch, H.W., 2012. Extraction of lignins from aqueous–ionic liquid mixtures by organic solvents. Biotechnol. Bioeng. 109, 346-352.

Zavrel, M., Bross, D., Funke, M., Büchs, J., Spiess, A.C., 2009. High-throughput screening for ionic liquids dissolving (ligno-)cellulose. Bioresour. Technol. 100, 2580-2587.

Zhang, H., Wu, J., Zhang, J., He, J., 2005. 1-Allyl-3-methylimidazolium Chloride Room Temperature Ionic Liquid: A New and Powerful Nonderivatizing Solvent for Cellulose. Macromolecules 38, 8272-8277.

Zhang, Y.H.P., Himmel, M.E., Mielenz, J.R., 2006. Outlook for cellulase improvement: Screening and selection strategies. Biotechnol. Adv. 24, 452-81.

Zhang, Y.H.P., Lynd, L.R., 2004. Toward an Aggregated Understanding of Enzymatic Hydrolysis of Cellulose: Noncomplexed Cellulase Systems. Biotechnol. Bioeng. 88, 797-824.

Zhao, H., Baker, G.A., Cowins, J.V., 2010. Fast Enzymatic Saccharification of Switchgrass After Pretreatment with Ionic Liquids. Biotechnol. Prog. 26, 127-133.

Zhao, H., Jones, C.I.L., Baker, G.A., Xia, S., Olubajo, O., Person, V.N., 2009. Regenerating cellulose from ionic liquids for an accelerated enzymatic hydrolysis. J. Biotechnol. 139, 47-54.

Zhu, S.D., Wu, Y.X., Chen, Q.M., Yu, Z.N., Wang, C.W., Jin, S.W., Ding, Y.G., Wu, G., 2006. Dissolution of cellulose with ionic liquids and its application: a mini-review. Green Chem. 8, 325-327.

Chapter 2

A model for optimizing the enzymatic hydrolysis of ionic liquid-pretreated lignocellulose

Abstract

Miscanthus x giganteus was pretreated with the ionic liquid (IL) 1-ethyl-3-methylimidazolium acetate at ten different pretreatment temperatures and times. The enzymatic hydrolysis of the pretreated *Miscanthus* to glucose and xylose was measured as a function of time to provide rate and final conversion data. A series of two irreversible, first-order reactions with Arrhenius temperature dependencies was used to model both the cellulose and hemicellulose pretreatment. This kinetic model was used to predict the enzymatic hydrolysis conversion of IL-pretreated *Miscanthus* over a range of pretreatment temperatures (70 - 140°C) and times (1 - 48 h), and indicated a wide range of optimal pretreatment conditions, from high temperatures/short times to lower temperatures/long times. Pre-exponential constants and activation energies obtained from the kinetic model are within reported ranges of experimentally obtained values for other pretreatments, indicating that the model may be broadly applicable to a variety of lignocellulosic pretreatment processes.

1. Introduction

1.1 Ionic liquid pretreatment

Several pretreatment methods have been developed to make biomass more amenable to enzymatic hydrolysis. A promising approach is biomass dissolution in ionic liquids (ILs) followed by the addition of an anti-solvent to precipitate the cellulosic fraction of the biomass prior to hydrolysis (Swatloski et al., 2002). One IL, 1-ethyl,3-methylimidizolium acetate ([C_2mim][OAc]) is very effective in pretreating a variety of lignocellulose substrates (Lee et al., 2009; Sun et al., 2009; Zavrel et al., 2009). The precipitated cellulose is reduced in crystalline content (Swatloski et al., 2002) and accessible to enzymatic hydrolysis (Shill et al., 2011).

1.2 Models of pretreatment processes

IL pretreatment conditions (e.g., time, temperature, biomass loading) significantly influence the effectiveness of enzymatic hydrolysis of pretreated biomass, and there is incomplete information about how these conditions alter the structure of lignocellulose. In contrast to pretreatments such as acid, ammonia, and steam, only a few studies have been performed to determine optimal IL pretreatment conditions for subsequent enzymatic hydrolysis (Arora et al., 2010; Fu and Mazza, 2011; Yoon et al., 2012). A number of variables impact downstream hydrolysis, such as pretreatment time, temperature, biomass loading, stirring, pressure, and water content. Performing an extensive study of all conditions is daunting, and design of experiments with accurate modeling is needed to understand this pretreatment parameter space. A subset of experiments can be performed to explore key pretreatment variables, and then the entire parameter space can be modeled. This has been undertaken using a polynomial fit to the data (Fu and Mazza, 2011; Silverstein et al., 2007). While this approach can be very useful for a particular subset of pretreatment conditions, little fundamental information is obtained, and therefore the model cannot be readily translated to different pretreatments.

1.3 Severity parameter and H-factor

An alternative approach to understanding pretreatment effectiveness employs a severity parameter (R_0), also known as the reaction ordinate or P-factor P_t, (Overend and Chornet, 1987) which indicates how severely the biomass has been pretreated and correlates to the ease of enzymatic hydrolysis of cellulose (Chum et al., 1988). This number reflects the relative reaction rate for the reactions that occur during pretreatment, and includes an Arrhenius dependency on pretreatment temperature. The severity parameter was originally derived from the H-factor, a measure of the relative delignification rate (Brasch and Free, 1965; Overend and Chornet, 1987), and both have been used by the pulp and paper industry to help understand and control temperature and time effects on the quality of pulp (Chum et al., 1990a; Vroom, 1957).

Pretreatment and acid hydrolysis kinetics have long been modeled with irreversible reaction kinetics (Lüers, 1930; Saeman, 1945). For both the severity parameter and H-factor, the pretreatment is modeled as a single step, irreversible reaction where

$$A \xrightarrow{k} B \tag{1}$$

represents biomass that undergoes hemicellulose, cellulose, and lignin solubilization and restructuring with the reaction rate k (Saville, 2011). The reaction is assumed to have an Arrhenius temperature dependence, resulting in a reaction rate of

$$\frac{-1}{C_A^n}\frac{dC_A}{dt} = k = A_0 \exp\left(\frac{-E_A}{RT}\right), \tag{2}$$

where C_A is the concentration of biomass any given time t (usually in minutes), A_0 is the pre-exponential factor (min^{-1}), E_A is the activation energy of the reaction (J/mol), R is the gas constant (8.314 J mol^{-1} K^{-1}), T the absolute reaction temperature (K), and n the order of the reaction (Garrote et al., 2002). The H-factor represents the ratio of the reaction rate to a reference reaction rate,

$$H = \int_0^t \frac{k}{k_r}dt = \int_0^t \exp\left(a - \frac{b}{T}\right)dt \text{ where } a = \frac{E_A}{RT_r}, b = \frac{E_A}{R}, \tag{3}$$

where k_r is the reaction rate at the reference temperature T_r (Jagannadh et al., 1993).

The severity parameter estimates the relative reaction rate instead by expanding to the second term of a Taylor series about T_r (Garrote et al., 2002), which then simplifies to

$$k = A_0 \exp\left(\frac{-E_A}{RT_r}\right)\exp\left(\frac{T-T_r}{\omega}\right), \text{ where } \omega = \frac{RT_r^2}{E_A}. \tag{4}$$

The severity parameter is defined as the ratio of the reaction rate, from equation 4, to the reference reaction rate, and simplifies to

$$R_O = \int_0^t \frac{k}{k_r}dt = \exp\left(\frac{T-T_r}{\omega}\right)t \tag{5}$$

after integration over time, where k_r is the reaction rate at the reference temperature T_r (Brasch and Free, 1965; Chum et al., 1990a; Garrote et al., 2002; Overend and Chornet, 1987). Most instances in the literature use T_r = 100°C, and ω = 14.75, which comes from the general approximation that a relative reaction rate doubles with an increase of 10°C in temperature (Brasch and Free, 1965; Vroom, 1957), resulting in

$$\ln(R_O) = \ln\left(2^{\left(\frac{T-100°\text{C}}{10°\text{C}}\right)}\right) = \frac{T-100°\text{C}}{\left(\frac{10°\text{C}}{\ln 2}\right)} \cong \frac{T-100°\text{C}}{14.75}. \tag{6}$$

While using a value of 14.75 in equation 5 works well on a variety of systems, this term should be modified to each system to account for differences in feedstock, pretreatment systems and reaction systems (Brasch and Free, 1965; Saville, 2011). Many modifications have also been made to the severity parameter to account for different pretreatments, such as the extended or combined severity parameter (CSF),

$$CSF = \log\left(R_O\left[\text{H}^+\right]\right) = \log R_O - pH, \tag{7}$$

which takes into account the hydrogen ion concentration $[\text{H}^+]$ as a reactant with species A to produce B, and has been used to predict severity for pretreatments involving acid as a reagent (e.g. organosolv, dilute acid) (Abatzoglou et al., 1992; Brosse et al., 2009; Chum et al., 1990a; Chum et al., 1990b; Schell et al., 2003).

Many groups have had success in correlating the severity parameter with ease of enzymatic degradation for a variety of pretreatment types (Chum et al., 1988; Kabel et al., 2007; Silverstein et al., 2007; Yang and Wyman, 2004). However, a severity parameter or H-factor approach has yet to be employed with ionic liquid pretreatment. Furthermore, neither parameter necessarily captures the product of interest for an IL pretreatment process. These one-step reaction schemes make it difficult to describe a primarily unreactive pretreatment process where the desired product is readily enzymatically degradable cellulose and hemicellulose.

1.4 Kinetic models for various biomass pretreatments

While a severity parameter or H-factor may be inappropriate for IL pretreatment, the concept of using a simplified reaction scheme has merit. A multistep kinetic model has been used successfully to model cellulose dissolution in phosphoric acid (Zhang et al., 2009). A similar approach has been successful in describing the kinetics of cellulose pyrolysis (Antal Jr. et al., 1998), dilute sulfuric acid pretreatment and hydrolysis (Blanch et al., 2011; Esteghlalian et al., 1997; Schell et al., 2003), cellulose hydrolysis by acids in ionic liquids (Binder and Raines, 2010; Dee and Bell, 2011a; Dee and Bell, 2011b; Li et al., 2008), and LiCl/DMAC cellulose dissolution (Marson and El Seoud, 1999; Ramos et al., 2005). In addition to a variety of pretreatments, different reaction schemes have been applied (Carrasco and Roy, 1992; Jacobsen and Wyman, 2000).

For example, Morinelly et al. (2009) employed the following reaction scheme for conversion of the xylan content in lignocellulose for dilute sulfuric acid pretreatment:

$$\text{Xylan} \xrightarrow{k_1} \text{Xylo-oligomers} \xrightarrow{k_2} \text{Xylose} \xrightarrow{k_3} \text{Furfural} \xrightarrow{k_4} \text{Degradation products} \tag{8}$$

This reaction was modeled as a series of irreversible reactions with first order dependence on acid concentration. Nine experiments were performed with varying acid concentrations and reaction temperatures, and the data were used to determine the acid dependence, pre-exponential, and activation energy parameters for each step (Morinelly et al., 2009). Although such simple kinetic models can predict experiments very well, more detailed models do exist that take into account different types of xylan, degradation pathways, and mass transfer to better describe the true mechanisms (Esteghlalian et al., 1997; Morinelly et al., 2009; Pronyk and Mazza, 2010). These types of reaction schemes may also be more suitable for characterizing ionic liquid pretreatment than the severity parameter.

1.5 A model for the effect of temperature and time on ionic liquid pretreatment

In the present work, a model was developed for determining the effectiveness of 1-ethyl, 3-methylimidzolium acetate ([C_2mim][OAc]) to pretreat *Miscanthus x giganteus*. [C_2mim][OAc] was chosen as the IL due to its previously studied ability to dissolve various forms of lignocellulose at high concentrations, its thermostability coupled with low melting temperature (< -20°C), its low viscosity, and its low toxicity and corrosiveness compared to other ILs (Sun et al., 2009). While there are many factors that can affect pretreatment effectiveness, time and temperature where chosen as the first variables to be studied because of their known effects on other pretreatment processes and the ease by which their impact can be modeled.

Pretreatment time and temperature were varied to determine optimum pretreatment conditions and calculate kinetic constants. Ten different pretreatments were performed at different temperatures for varying lengths of time, and enzymatic hydrolysis was conducted afterwards, measuring the conversion to glucose and xylose. Modeling the process as a two-step, irreversible series reaction enabled the prediction of the enzymatic hydrolysis conversion for the entire IL pretreatment time and temperature space. This model was applied to both cellulose and hemicellulose pretreatment and enzymatic conversion processes. The model improves upon the severity parameter approach by proposing a reaction scheme where the desired product is enzymatically-degradable polysaccharides.

2. Materials and Methods

2.1 Materials

Ionic liquids. [C_2mim][OAc] was purchased from IOLITEC (IL-0189-TG-1000, >95% pure), and used without further purification or drying.

Cellulase enzymes. A cellulase cocktail from *Trichoderma reesei* (Celluclast 1.5L, Product # C2730-50ml) and β-glucosidase (Novo188 Product # C6105-50ml) were purchased from Sigma Aldrich. The activity of the Celluclast 1.5L was reported to be 800 EGU/g, and of Novo188 to be 258 CBU/g. The IUPAC Filter Paper Assay (Ghose, 1987) was performed for Celluclast 1.5L and the activity of the enzyme mixture was found to be 115 FPU/mL of solution.

Substrates. *Miscanthus x giganteus* from the University of Illinois, Urbana-Champaign was ground and placed through a 4mm particle size sieve plate, yielding a heterogeneous mixture of particles up to 1cm in length. The cellulose, hemicellulose (primarily xylan), lignin, and water content of the *Miscanthus* were determined by compositional analysis (Sluiter et al., 2008), and are shown in Figure 1. *Miscanthus* was chosen as a promising feedstock for biofuel production because it does not compete with food sources and is easy to cultivate (Brosse et al., 2009; Somerville et al., 2010).

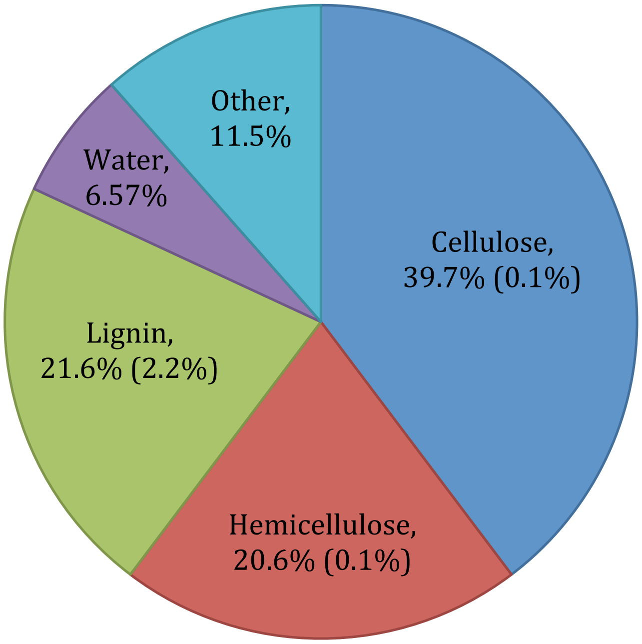

Figure 1. Compositional analysis of *Miscanthus*. Values in parentheses show one standard deviation in error.

2.2 Pretreatment

Pretreatment time and temperature were varied from 1-48 h and from 70°C-140°C, respectively. A minimum time of 1 h was chosen to ensure that heating and mixing effects were minimized, and a maximum time of 48 h was chosen to ensure industrially relevant pretreatment times. A temperature of greater than 70°C was used to reduce viscosity and mixing effects, and the maximum temperature of 140°C was chosen to prevent thermal degradation of the ionic liquid (Li et al., 2011). Table 1 shows the pretreatment conditions that were examined experimentally.

[Emim][OAc] (25 g) was heated in a beaker in a silicone oil bath to the desired pretreatment temperature (70°C-140°C). After reaching the desired temperature, 1 g of *Miscanthus* was added. The mixture was stirred for the desired pretreatment time (1-48 h), then removed from the oil bath to cool down to 80°C while stirring. The heating and cooling times are not included in the pretreatment time. Once the mixture was at 80°C (or immediately for lower than 80°C conditions), 25 g of 80°C water was added to precipitate the biomass. The water was preheated to help minimize gel formation for easier precipitation, while keeping the temperature low enough to prevent boiling, which might have impacted the biomass. The IL/water/biomass mixture was centrifuged for 5 min at 3220 x g, and the supernatant removed with a syringe. Citrate buffer (50 mM, pH 4.8) was added to replenish the volume to 50 mL total, and the mixture was vortexed to wash the solids. The mixture was centrifuged and washed again twice more to remove IL from the solids and ensure the mixture was at pH 4.8 before being hydrolyzed. All pretreatments were performed in duplicate.

2.3 Enzymatic hydrolysis

The washed, pretreated *Miscanthus* was placed in a 125-mL Erlenmeyer flask with additional citrate buffer for a total mass of 50 g (Shill et al., 2011). Since a mass balance was not performed in between pretreatment and hydrolysis, all enzymatic conversions represent overall process conversions and account for any cellulose or hemicellulose lost during pretreatment. Duplicate pretreatment samples were hydrolyzed separately to help reduce the effects of substrate heterogeneity. The mixture was heated to 50°C in an incubating orbital shaker, and then 0.0625 mL each of Celluclast 1.5L and Novo188 (for excess β-glucosidase) was added. The mixture was shaken at 250 rpm, and well-mixed 0.5-mL samples were removed at desired time intervals until hydrolysis was complete (after 5 days). The samples were analyzed for glucose and xylose concentration using a YSI 2700 Select Biochemistry Analyzer, with each sample analyzed in duplicate. This results in four concentration values that were averaged for each conversion data point, and allows for standard deviation calculations. The percent conversion for the cellulose portion was calculated by

$$\begin{aligned}\text{Percent conversion} &= \frac{\text{Glucose conc}\left(g/mL\right)\times\text{reaction vol }\left(mL\right)}{\text{biomass }\left(g\right)\times\text{wt\% cellulose in biomass}}\\ &\quad\times\frac{162\text{ (MW of cellulose unit)}}{180\text{ (MW of glucose unit)}}\times 100,\end{aligned} \tag{9}$$

and is based on the mass of *Miscanthus* used before pretreatment, thus representing an overall process conversion. The conversion of the hemicellulose portion to xylose was calculated similarly by

$$\text{Percent conversion} = \frac{\text{Xylose conc}(g/mL)\times\text{reaction vol }(mL)}{\text{biomass }(g)\times\text{wt\% xylan in biomass}} \times\frac{132\text{ (MW of xylan unit)}}{150\text{ (MW of xylose unit)}}\times 100, \tag{10}$$

and is based on the difference in molecular weight between xylan, the primary component of hemicellulose in *Miscanthus*, and xylose unit.

2.4 IL pretreatment model

Several assumptions were used to model the dissolution of *Miscanthus* in [C_2mim][OAc]. Pseudo-first order kinetics were assumed for simplicity. Pretreatment was assumed to follow a reaction path of

$$A\xrightarrow{k_1}B\xrightarrow{k_2}C\ , \tag{11}$$

where A represents the cellulose component of lignocellulosic biomass, B represents enzymatically-accessible cellulose, and C represents degradation products. The reaction A⟶B represents the conversion of cellulase-inaccessible cellulose to cellulase-accessible cellulose, which is accomplished by a variety of mechanisms, such as decrystallization of the cellulose structure, removal/rearrangement of lignin, and the swelling of cell walls. The reaction B⟶C represents further degradation to undesirable waste products, either through chemical or thermal degradation pathways. Product C includes insoluble degradation products (e.g. humins) as well as any soluble product that would be lost during subsequent washes (e.g. soluble oligomers, glucose monomers, 5-hydroxymethyl furfural).

An analogous set of reactions was assumed for hemicellulose, with the exception that hemicellulose inaccessibility is not due to crystallinity, but rather the presence of lignin, which hinders enzymatic breakdown of both cellulose and hemicellulose. In this case the reaction of A⟶B represents the solvation of lignin by IL to expose hemicellulose to hemicellulases, and B⟶C represents the degradation of hemicellulose to soluble products or humins.

The rate constants for equation 11 were assumed to follow the Arrhenius form:

$$k_1 = A_1\exp\left(\frac{-E_{A1}}{RT}\right),\text{ and }k_2 = A_2\exp\left(\frac{-E_{A2}}{RT}\right), \tag{12}$$

where A_1 and A_2 are pre-exponential constants (h^{-1}), E_{A1} and E_{A2} are activation energies (J/mol), R is the gas constant (8.314 J mol^{-1} K^{-1}), and T is the absolute reaction temperature (K). The first-order, irreversible reactions of equation 11 can thus be modeled to provide the time course of formation of B:

$$\text{Percent final conversion} = \frac{[B]}{[A_0]}\times 100 = \frac{k_1}{k_2-k_1}\left(\exp(-k_1t)-\exp(-k_2t)\right)\times 100\ , \tag{13}$$

where [B] is the concentration of enzymatically hydrolyzed cellulose, [A_0] is the starting concentration of cellulose in the biomass, and t (h) is the pretreatment time. Percent final conversion is defined by equation 9, using the final glucose concentration (after 5 days of hydrolysis). Equation 13 was used to model the pretreatment time-temperature space, and the percent final conversion used to fit the Arrhenius parameters for each step. Once the rate constants were obtained, the constants were used to predict the conversion for the entire pretreatment time-temperature space.

2.5 Parameter estimation

Determining the Arrhenius parameters required fitting two unknowns for each reaction step (pre-exponential constant and activation energy) for each data set. The 2011 Excel Solver package from Frontline Systems was used to determine the best fit of the four variables. The fitted parameters were sensitive to initial guess values, so an alternative approach was also developed to verify the Excel results. A MATLAB solver was programmed to minimize the nonlinear multivariable least squares fit for an array of initial guesses, and select the parameters that resulted in the smallest residual error.

3. Results and Discussion

3.1 Time course results

For each of the experimental pretreatment conditions, enzymatic hydrolysis was performed and sugar concentrations were measured as a function of time. Figures 2 and 3 show select hydrolysis time-course data for various pretreatment conditions. Table 1 shows the final cellulose and hemicellulose conversions obtained with enzymatic hydrolysis for all of the experimental pretreatment conditions.

Figure 2 (pretreatment time of 48 h) illustrates that the enzymatic conversion increased with increasing pretreatment temperature until a maximum was reached, and then the conversion decreased with increasing temperature, most likely due to degradation of cellulose to either insoluble byproducts or soluble molecules that are washed away before hydrolysis. All other enzymatic hydrolysis time-course data for cellulose conversion to glucose are provided in the Appendix.

Figure 3 shows select data for the enzymatic hydrolysis of hemicellulose to xylose, using the native hemicellulase activity of the Celluclast 1.5L. These data were obtained concurrently with the glucose data, with both hydrolyses occurring simultaneously. Figure 3 illustrates the effect of pretreatment temperature for a pretreatment time of 1 h. Further enzymatic hydrolysis data for other pretreatment conditions are included in the Appendix. Hemicellulose, which is less recalcitrant than cellulose, is generally more reactive than cellulose (Lynd, 1996), and thus requires different optimal pretreatment conditions than cellulose. The enzymatic hydrolyses of hemicellulose pretreated with [C_2mim][OAc] is thus unable to attain complete conversion, as some of the hemicellulose is either degraded or washed away (Shill et al., 2011). To further optimize hemicellulose hydrolysis, the washing process would need to be further studied in addition to using less severe [C_2mim][OAc] pretreatment conditions.

Pretreatment time, h	**Pretreatment temperature, °C**	**Final cellulose conversion, %**	**Final hemicellulose conversion, %**
1	70	9.31 (0.069)	3.33 (1.10)
1	100	34.7 (0.809)	18.9 (0.668)
1	120	86.3 (0.419)	50.2 (2.84)
1	140	91.7 (0.921)	40.9 (0.975)
2	140	83.7 (1.92)	18.1 (0.696)
24	100	86.7 (2.55)	46.0 (1.98)
48	70	54.2 (4.68)	29.5 (5.14)
48	100	90.0 (1.09)	36.1 (1.29)
48	120	74.0 (3.14)	22.8 (2.12)
48	140	50.9 (2.68)	10.6 (1.07)

Table 1. Experimental ionic liquid pretreatment times and temperatures, and the final enzymatic conversions of cellulose and hemicellulose. Values in parentheses show one standard deviation in error.

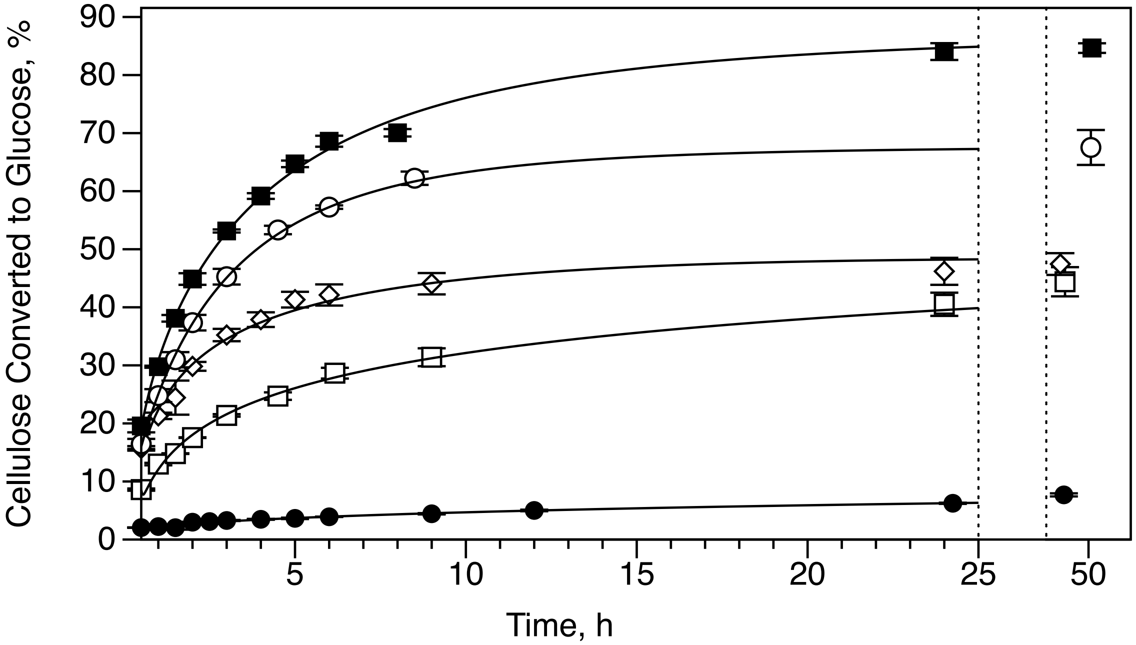

Figure 2. Enzymatic conversion of *Miscanthus* to glucose as a function of time. Ionic liquid pretreatment temperatures were varied (□: 70°C, ■: 100°C, ○: 120°C, ◇: 140°C) with a constant pretreatment time of 48 h. The enzymatic hydrolysis of untreated *Miscanthus* (●) is shown for comparison. Error bars represent one standard deviation.

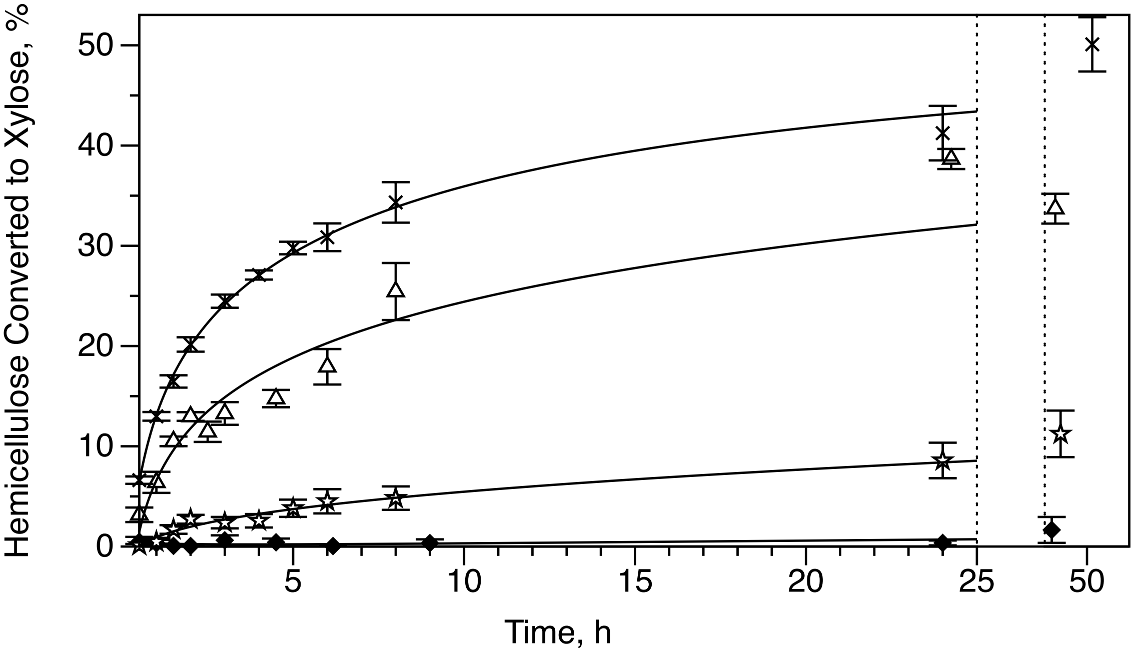

Figure 3. Enzymatic conversion of *Miscanthus* to xylose as a function of time. Ionic liquid pretreatment temperatures were varied (◆: 70°C, ☆: 100°C, ✕: 120°C, △: 140°C) with a constant pretreatment time of 1 h. Error bars represent one standard deviation.

3.2 Kinetic pretreatment model

The pre-exponential and activation energies of the pretreatment model were determined from the experimental data in Table 1, and the resulting parameters are shown in Table 2. The R^2 of 0.95 for the cellulose pretreatment indicates a good fit of the data to the model. The model was then extrapolated over the full time (1 - 48h) and temperature range (70-140°C) to calculate the cellulose conversion at all possible pretreatment conditions. These results, compared to the experimental values (blue dots), are shown in Figure 4, as well as in contour form in the Appendix.

The pretreatment behavior for cellulose in Figure 4 indicates a wide range of pretreatment conditions (light yellow portion) that result in high final cellulose conversions, from high temperatures/short times to lower temperatures/long times. The model also shows the regions of pretreatment conditions that result in under-pretreatment (lower temperatures/short times), in which cellulose is not rendered adequately accessible, and over-pretreatment (high temperatures/long times), in which degradation products are formed. These results have clear economic and processing implications, and offer a wide range of options for tuning the pretreatment conditions to meet the requirements of a desired process.

The hemicellulose conversion was similarly analyzed and its kinetic parameters and R^2 value are also provided in Table 2. The R^2 of 0.61 for this model indicates a positive correlation, but does not fit the experimental values as well as the cellulose model. This poorer fit may be due to the more frequent loss of hemicellulose during the washing phases. A detailed mass balance for the process, in addition to an optimized washing process, is needed to better understand the details of hemicellulose pretreatment and to refine and improve the model. Since only ten pretreatment conditions were performed experimentally, additional experimentation at other pretreatment conditions may be needed to help improve and verify the hemicellulose and cellulose models.

The extrapolated hemicellulose conversion for the entire pretreatment space is shown in Figure 5, along with the experimental values (blue dots). The pretreatment behavior for hemicellulose also indicates a wide range of pretreatment conditions that give favorable hemicellulose conversions. The conditions are shifted to shorter times and lower temperatures than for cellulose conversion, indicating that hemicellulose is more susceptible to over-pretreatment than the cellulose portion of *Miscanthus*. The Appendix also contains a contour plot of the hemicellulose conversion model.

Arrhenius parameter	Cellulose model	Hemicellulose model
A_1 h^{-1}	6.6×10^{14}	7.8×10^{13}
E_{A1} J/mol	1.1×10^{5}	1.1×10^{5}
A_2 h^{-1}	3.9×10^{4}	2.4×10^{14}
E_{A2} J/mol	5.1×10^{4}	1.1×10^{5}
R^2	0.95	0.61

Table 2. Kinetic model parameters for cellulose and hemicellulose conversion.

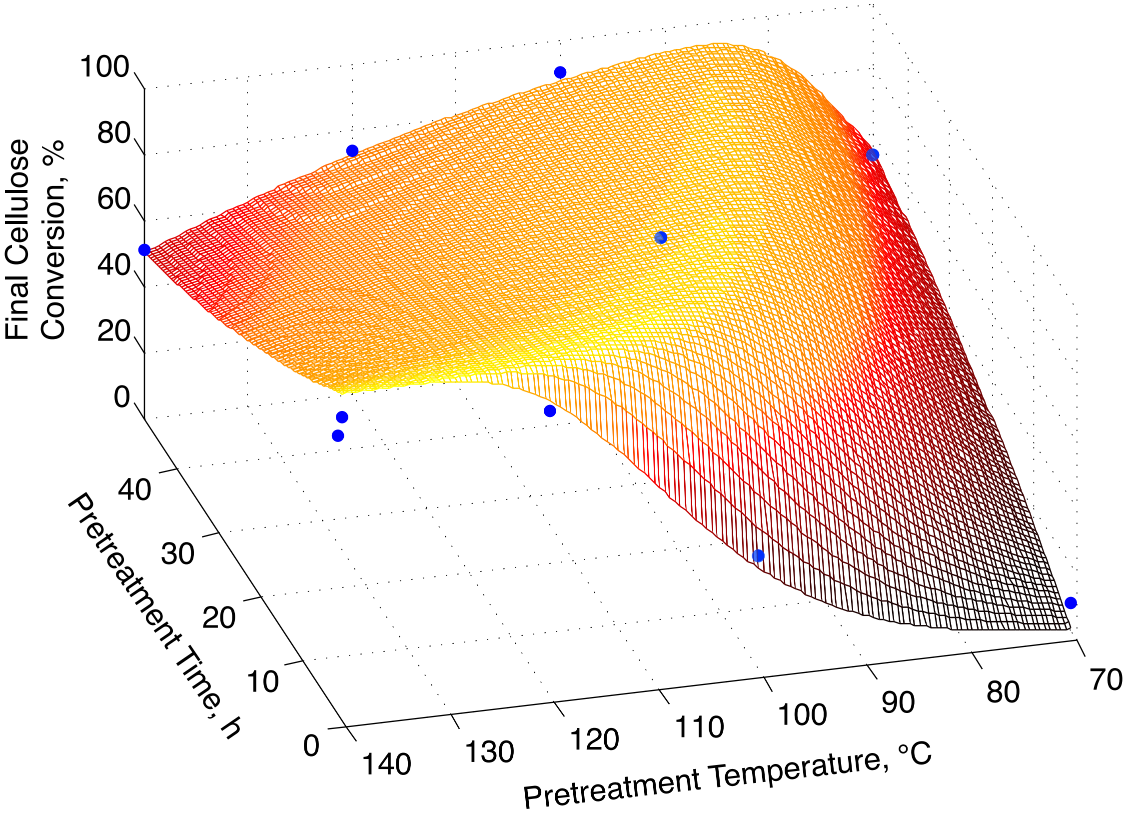

Figure 4. Final cellulose conversion modeled as a function of pretreatment temperature and pretreatment time (red-yellow mesh) compared to experimental hydrolysis data (blue points).

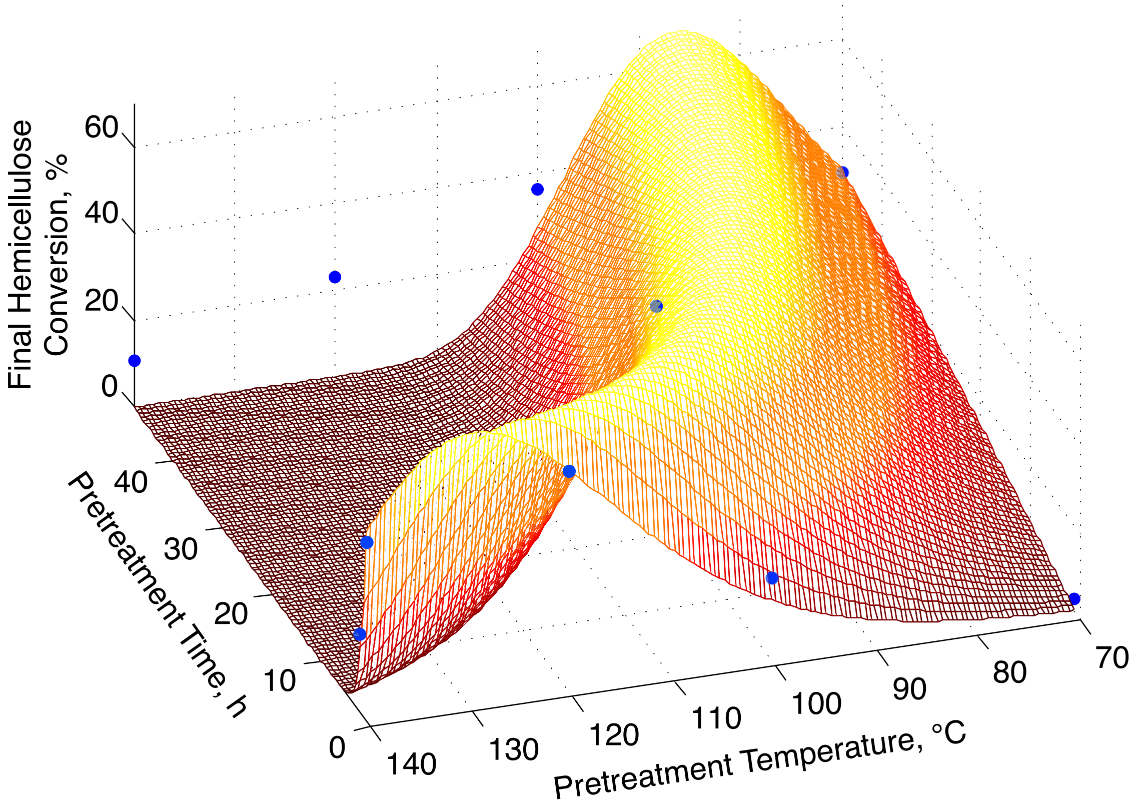

Figure 5. Final hemicellulose conversion modeled as a function of pretreatment temperature and pretreatment time (red-yellow mesh) compared to experimental data (blue points).

3.3 Polynomial fit model

The present kinetic model was compared to an arbitrary multivariable polynomial model of the form $\%Conversion = a + b_1 t + b_2 T + c_1 t^2 + c_2 T^2 + dtT$, which was used to fit IL pretreatment by Fu and Mazza (2011). The experimental data were fit to the polynomial model by varying the six parameters and minimizing the sum of the residuals, giving an R^2 of 0.87 (parameters are shown in the Appendix). The proposed kinetic model fits the experimental data better than the polynomial fit, indicating that the kinetic model better captures the behavior of the system with fewer fitted parameters. In addition, the fitted parameters from the kinetic model have physical meaning, rather than being purely empirical parameters.

The hemicellulose data was also analyzed using the polynomial model, resulting in an R^2 of 0.71 (parameters are shown in the Appendix). The polynomial model performs slightly better than the proposed kinetic model. While the kinetic model still has fewer variables, its poorer fit of the hemicellulose data reiterates the need for additional experimentation and optimization.

3.4 Evaluation of kinetic parameters

The kinetic pretreatment analysis provides a mechanistic model that not only accurately defines the pretreatment time-temperature space for enzyme digestibility, but also gives fundamental insights into some of the mechanisms for effective pretreatment. This can be confirmed by comparing the values obtained from the model to experimentally determined values reported for similar systems in the literature, shown in Tables 3 (cellulose) and 4 (hemicellulose). Many of the parameters have a large range of values due to the models' sensitivities to biomass composition and process conditions (Lin et al., 2009).

In Table 3, A_1 and E_{A1} are compared to delignification or rearrangement of the biomass (Li et al., 2002), as well as to decrystallization/dissolution of cellulose (Zhang et al., 2009). A_2 and E_{A2} are compared to cellulose and glucose degradation (Dee and Bell, 2011a; Dee and Bell, 2011b; Lin et al., 2009). In addition, E_{A1} is compared to calculations from molecular dynamic simulations (Gross and Chu, 2010). Here, E_{A1} is equivalent to the energy to break the hydrogen bonds needed to liberate a cellulose unit on the surface (calculation in the Appendix). While an oversimplification for this complex system, this comparison helps provide insights into the IL pretreatment process, and supports the hypothesis that a major element of the IL pretreatment mechanism is decrystallization of cellulose.

In Table 4, A_1 and E_{A1} are compared to delignification or rearrangement of the biomass (Tunc et al., 2010), and A_2 and E_{A2} are compared to xylan hydrolysis and degradation (Carrasco and Roy, 1992; Dee and Bell, 2011a).

Arrhenius Parameter	**This work (cellulose)**	**Delignification and Degradation of Cellulose by Pulping methods (Li et al., 2002)**	**Cellulose dissolution by phosphoric acid (Zhang et al., 2009)**	**Acid hydrolysis of *Miscanthus* in BmimCl (Dee and Bell, 2011a)**	**Energy to liberate a cellulose unit (Gross and Chu, 2010)**	**Pyrolysis (Lin et al., 2009)**
A_1 h^{-1}	6.6×10^{14}	3×10^{13} - 2.6×10^{15}	1.2×10^{6}			
E_{A1} J/mol	1.1×10^{5}	$1.2 - 1.4 \times 10^{5}$	4.2×10^{4}		1.0×10^{5}	
A_2 h^{-1}	3.9×10^{4}	5.6×10^{18} - 5.8×10^{20}				3.6×10^{5} – 1.3×10^{21}
E_{A2} J/mol	5.1×10^{4}	$1.7 - 1.9 \times 10^{5}$		9.5×10^{4}		4.8×10^{4} – 2.8×10^{5}

Table 3. Kinetic parameters obtained by modeling IL-pretreated cellulose hydrolysis compared to experimental values from the literature.

Arrhenius Parameter	**This work (hemi-cellulose)**	**Acid hydrolysis of *Miscanthus* in BmimCl (Dee and Bell, 2011a)**	**Hemicellulose autohydrolysis (Tunc et al., 2010)**	**Xylose degradation in dilute acid (Carrasco and Roy, 1992)**
A_1 h^{-1}	7.8×10^{13}			
E_{A1} J/mol	1.1×10^{5}		1.3×10^{5}	
A_2 h^{-1}	2.4×10^{14}			4.3×10^{12}- 9×10^{16}
E_{A2} J/mol	1.1×10^{5}	1.1×10^{5}		1.0- 1.4×10^{5}

Table 4. Kinetic model parameters obtained by modeling IL-pretreated hemicellulose hydrolysis compared to experimental values from the literature.

While the kinetic pretreatment model is a simplification of the complex process of IL pretreatment, that the obtained values fall within ranges obtained through a variety of different methods and pretreatments helps validate the model's broad application to pretreatment processes. Given the large number of pretreatment processes, including IL processes, this type of analysis should prove useful in minimizing experimental data needed to determine optimal pretreatment conditions. In addition, fundamental insights from this type of analysis could be applied in a cheminformatics approach to select an optimal IL from the vast number of possible candidates. Better understanding of the dissolution mechanism of biomass in ILs, from both experimental and computational methods, will yield further improvements in mechanistic models and enable further optimization of pretreatment conditions for enzymatic hydrolysis.

4. Conclusions

Miscanthus x giganteus was pretreated with the ionic liquid [C_2mim][OAc] over a range of temperatures and times to determine the pretreatment effectiveness for enzymatic hydrolysis. The IL pretreatment was successfully modeled by a two-step series of irreversible first-order reactions governed by an Arrhenius dependence on temperature. This model was used to predict and optimize the enzymatic hydrolysis conversion for a range of IL pretreatment conditions, as well as obtain kinetic parameters for the reactions involved. The model and parameters obtained should prove useful in optimizing future IL pretreatment processes, as well as understanding the IL pretreatment mechanism.

Acknowledgements

This work was funded by the Energy Biosciences Institute. We thank Mahmoud K. F. Abouelnasr for helpful discussions.

References

Abatzoglou, N., Chornet, E., Belkacemi, K., Overend, R.P., 1992. Phenomenological Kinetics of Complex Systems: The Development of a Generalized Severity Parameter and its Application to Lignocellulosic Fractionation. Chem. Eng. Sci. 47, 1109-1122.

Antal Jr., M.J., Várhegyi, G., Jakab, E., 1998. Cellulose Pyrolysis Kinetics: Revisited. Ind. Eng. Chem. Res. 37, 1267-1275.

Arora, R., Manisseri, C., Li, C., Ong, M.D., Scheller, H.V., Vogel, K., Simmons, B.A., Singh, S., 2010. Monitoring and Analyzing Process Streams Towards Understanding Ionic Liquid Pretreatment of Switchgrass (*Panicum virgatum* L.). Bioenerg. Res. 3, 134-145.

Binder, J.B., Raines, R.T., 2010. Fermentable sugars by chemical hydrolysis of biomass. Proc. Natl. Acad. Sci. U. S. A. 107, 4516-4521.

Blanch, H.W., Simmons, B.A., Klein-Marcuschamer, D., 2011. Biomass deconstruction to sugars. Biotechnol. J. 6, 1-17.

Brasch, D.J., Free, K.W., 1965. Prehydrolysis-Kraft Pulping of Pinus radiata Grown in New Zealand. Tappi 48, 245-248.

Brosse, N., Sannigrahi, P., Ragauskas, A., 2009. Pretreatment of Miscanthus x giganteus Using the Ethanol Organosolv Process for Ethanol Production. Ind. Eng. Chem. Res. 48, 8328-8334.

Carrasco, F., Roy, C., 1992. Kinetic study of dilute-acid prehydrolysis of xylan-containing biomass. Wood Sci. Technol. 26, 189-208.

Chum, H.L., Johnson, D.K., Black, S., Baker, J., Grohmann, K., Sarkanen, K.V., Wallace, K., Schroeder, H.A., 1988. Organosolv Pretreatment for Enzymatic Hydrolysis of Poplars: 1. Enzyme Hydrolysis of Cellulosic Residues. Biotechnol. Bioeng. 31, 643-649.

Chum, H.L., Johnson, D.K., Black, S.K., 1990a. Organosolv Pretreatment for Enzymatic Hydrolysis of Poplars. 2. Catalyst Effects and the Combined Severity Parameter. Ind. Eng. Chem. Res. 29, 156-162.

Chum, H.L., Johnson, D.K., Black, S.K., Overend, R.P., 1990b. Pretreatment-Catalyst effects and the combined severity parameter. Appl. Biochem. Biotechnol. 24/25, 1-14.

Dee, S., Bell, A.T., 2011a. Effects of reaction conditions on the acid-catalyzed hydrolysis of miscanthus dissolved in an ionic liquid. Green Chem. 13, 1467-1475.

Dee, S.J., Bell, A.T., 2011b. A Study of the Acid-Catalyzed Hydrolysis of Cellulose Dissolved in Ionic Liquids and the Factors Influencing the Dehydration of Glucose and the Formation of Humins. ChemSusChem 4, 1166-1173.

Esteghlalian, A., Hashimoto, A.G., Fenske, J.J., Penner, M.H., 1997. Modeling and Optimization of the Dilute-Sulfuric-Acid Pretreatment of Corn Stover, Poplar and Switchgrass. Bioresour. Technol. 59, 129-136.

Fu, D., Mazza, G., 2011. Aqueous ionic liquid pretreatment of straw. Bioresour. Technol. 102, 7008-7011.

Garrote, G., Domínguez, H., Parajó, J.C., 2002. Interpretation of deacetylation and hemicellulose hydrolysis during hydrothermal treatments on the basis of the severity factor. Process Biochem. 37, 1067-1073.

Ghose, T.K., 1987. Measurement of Cellulase Activities. Pure Appl. Chem. 59, 257-268.

Gross, A.S., Chu, J.-W., 2010. On the Molecular Origins of Biomass Recalcitrance: The Interaction Network and Solvation Structures of Cellulose Microfibrils. J. Phys. Chem. B 114, 13333-13341.

Jacobsen, S.E., Wyman, C.E., 2000. Cellulose and hemicellulose hydrolysis models for application to current and novel pretreatment processes. Appl. Biochem. Biotechnol. 84-86, 81-96.

Jagannadh, S.V.N., Hart, P.W., Hsieh, J.S., 1993. An analytical equation for H-factor using the entering liquor temperature as a variable. Tappi J. 76, 75-76.

Kabel, M.A., Bos, G., Zeevalking, J., Voragen, A.G.J., Schols, H.A., 2007. Effect of pretreatment severity on xylan solubility and enzymatic breakdown of the remaining cellulose from wheat straw. Bioresour. Technol. 98, 2034-2042.

Lee, S.H., Doherty, T.V., Linhardt, R.J., Dordick, J.S., 2009. Ionic Liquid-Mediated Selective Extraction of Lignin From Wood Leading to Enhanced Enzymatic Cellulose Hydrolysis. Biotechnol. Bioeng. 102, 1368-1376.

Li, C., Wang, Q., Zhao, Z.K., 2008. Acid in ionic liquid: An efficient system for hydrolysis of lignocellulose. Green Chem. 10, 177-182.

Li, W., Sun, N., Stoner, B., Jiang, X., Lu, X., Rogers, R.D., 2011. Rapid dissolution of lignocellulosic biomass in ionic liquids using temperatures above the glass transition of lignin. Green Chem. 13, 2038.

Li, Z., Li, J., Kubes, G.J., 2002. Kinetics of delignification and cellulose degradation during kraft pulping with polysulphide and anthraquinone. J. Pulp Pap. Sci. 28, 234-239.

Lin, Y.-C., Cho, J., Tompsett, G.A., Westmoreland, P.R., Huber, G.W., 2009. Kinetics and Mechanism of Cellulose Pyrolysis. J. Phys. Chem. C 113, 20097-20107.

Lüers, H., 1930. Das Celluloseverzuckerungsverfahren von H. Scholler. Z. Angew. Chem. 43, 455-458.

Lynd, L.R., 1996. Overview and Evaluation of Fuel Ethanol From Cellulosic Biomass: Technology, Economics, the Environment, and Policy. Annu. Rev. Energy Environ. 21, 403-465.

Marson, G.A., El Seoud, O.A., 1999. Cellulose dissolution in lithium chloride/ N,N-dimethylacetamide solvent system: Relevance of kinetics of decrystallization to cellulose derivatization under homogeneous solution conditions. J. Polym. Sci., Part A: Polym. Chem. 37, 3738-3744.

Morinelly, J.E., Jensen, J.R., Browne, M., Co, T.B., Shonnard, D.R., 2009. Kinetic Characterization of Xylose Monomer and Oligomer Concentrations during Dilute Acid Pretreatment of Lignocellulosic Biomass from Forests and Switchgrass. Ind. Eng. Chem. Res. 48, 9877-9884.

Overend, R.P., Chornet, E., 1987. Fractionation of lignocellulosics by steam-aqueous pretreatments. Philos. Trans. R. Soc. London, A 321, 523-536.

Pronyk, C., Mazza, G., 2010. Kinetic Modeling of Hemicellulose Hydrolysis from Triticale Straw in a Pressurized Low Polarity Water Flow-Through Reactor. Ind. Eng. Chem. Res. 49, 6367-6375.

Ramos, L.A., Assaf, J.M., El Seoud, O.A., Frollini, E., 2005. Influence of the Supramolecular Structure and Physicochemical Properties of Cellulose on Its Dissolution in a Lithium Chloride/ N,N-Dimethylacetamide Solvent System. Biomacromolecules 6, 2638-2647.

Saeman, J.F., 1945. Kinetics of Wood Saccharification: Hydrolysis of Cellulose and Decomposition of Sugars in Dilute Acid at High Temperature. Ind. Eng. Chem. 37, 43-52.

Saville, B.A., 2011. Pretreatment Options, in: Hood, E.E., Nelson, P., Powell, R. (Eds.), Plant Biomass Conversion, First ed. John Wiley & Sons Inc., West Sussex, UK, pp. 199-226.

Schell, D.J., Farmer, J., Newman, M., McMillan, J.D., 2003. Dilute–Sulfuric Acid Pretreatment of Corn Stover in Pilot-Scale Reactor. Appl. Biochem. Biotechnol. 105-108, 69-85.

Shill, K., Padmanabhan, S., Xin, Q., Prausnitz, J.M., Clark, D.S., Blanch, H.W., 2011. Ionic liquid pretreatment of cellulosic biomass: Enzymatic hydrolysis and ionic liquid recycle. Biotechnol. Bioeng. 108, 511-520.

Silverstein, R.A., Chen, Y., Sharma-Shivappa, R.R., Boyette, M.D., Osborne, J., 2007. A comparison of chemical pretreatment methods for improving saccharification of cotton stalks. Bioresour. Technol. 98, 3000-3011.

Sluiter, A., Hames, B., Ruiz, R., Scarlata, C., Sluiter, J., Templeton, D., Crocker, D. 2008. Determination of Structural Carbohydrates and Lignin in Biomass. National Renewable Energy Laboratory. NREL/TP-510-42618.

Somerville, C., Youngs, H., Taylor, C., Davis, S.C., Long, S.P., 2010. Feedstocks for Lignocellulosic Biofuels. Science 329, 790-792.

Sun, N., Rahman, M., Qin, Y., Maxim, M.L., Rodríguez, H., Rogers, R.D., 2009. Complete dissolution and partial delignification of wood in the ionic liquid 1-ethyl-3-methylimidazolium acetate. Green Chem. 11, 646-655.

Swatloski, R.P., Spear, S.K., Holbrey, J.D., Rogers, R.D., 2002. Dissolution of Cellose with Ionic Liquids. J. Am. Chem. Soc. 124, 4974-4975.

Tunc, M.S., Lawoko, M., van Heiningen, A., 2010. Understanding the Limitations of Removal of Hemicelluloses During Autohydrolysis of a Mixture of Southern Hardwoods. BioResources 5, 356-371.

Vroom, K.E., 1957. The "H" Factor: A Means of Experessing Cooking Times and Temperatures as a Single Variable. Pulp Paper Mag. Can. 58, 228-231.

Yang, B., Wyman, C.E., 2004. Effect of xylan and lignin removal by batch and flowthrough pretreatment on the enzymatic digestibility of corn stover cellulose. Biotechnol. Bioeng. 86, 88-95.

Yoon, L.W., Ang, T.N., Ngoh, G.C., Chua, A.S.M., 2012. Regression analysis on ionic liquid pretreatment of sugarcane bagasse and assessment of structural changes. Biomass Bioenergy 36, 160-169.

Zavrel, M., Bross, D., Funke, M., Büchs, J., Spiess, A.C., 2009. High-throughput screening for ionic liquids dissolving (ligno-)cellulose. Bioresour. Technol. 100, 2580-2587.

Zhang, J., Zhang, J., Lin, L., Chen, T., Zhang, J., Liu, S., Li, Z., Ouyang, P., 2009. Dissolution of Microcrystalline Cellulose in Phosphoric Acid—Molecular Changes and Kinetics. Molecules 14, 5027-5041.

Appendix

Polynomial parameter	This work (cellulose)	Fu and Mazza (2011) cellulose	This work (hemicellulose)
a	-2600	-1242	-1920
b_1	13	14	7.1
b_2	13	35	9.9
c_1	-0.036	-0.04	-0.022
c_2	-0.015	-2.5	-0.012
d	-0.028	-0.08	-0.016
R^2	0.87	0.94*	0.71

*The R2 value is for the time, temperature, and IL/water concentration model fit.

Table A1. Parameters found from polynomial fit, compared to literature values.

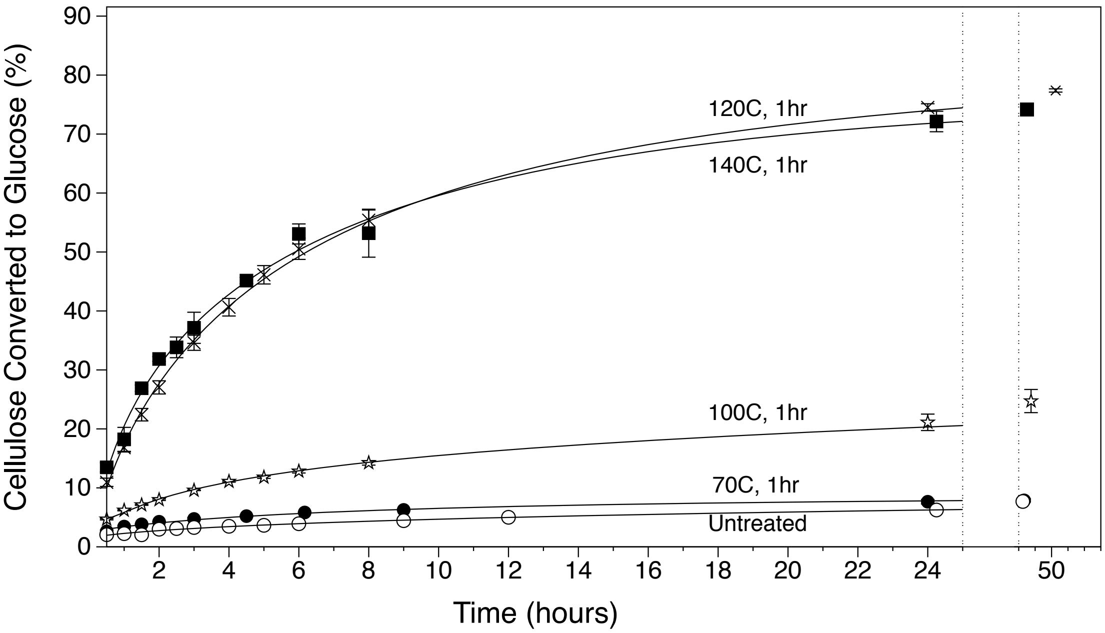

Figure A1. Enzymatic conversion of *Miscanthus* to glucose as a function of time. Ionic liquid pretreatment temperatures were varied with a constant pretreatment time of 1 h. The enzymatic hydrolysis of untreated Miscanthus is shown for comparison.

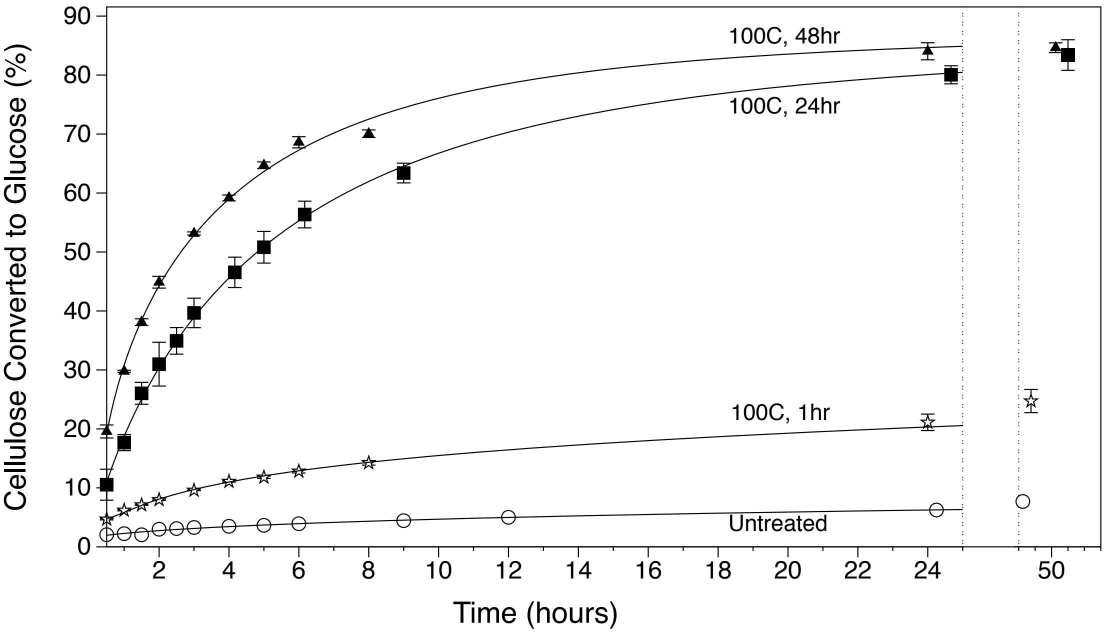

Figure A2. Enzymatic conversion of *Miscanthus* to glucose as a function of time. Ionic liquid pretreatment times were varied with a constant pretreatment temperature of 100°C. The enzymatic hydrolysis of untreated *Miscanthus* is shown for comparison.

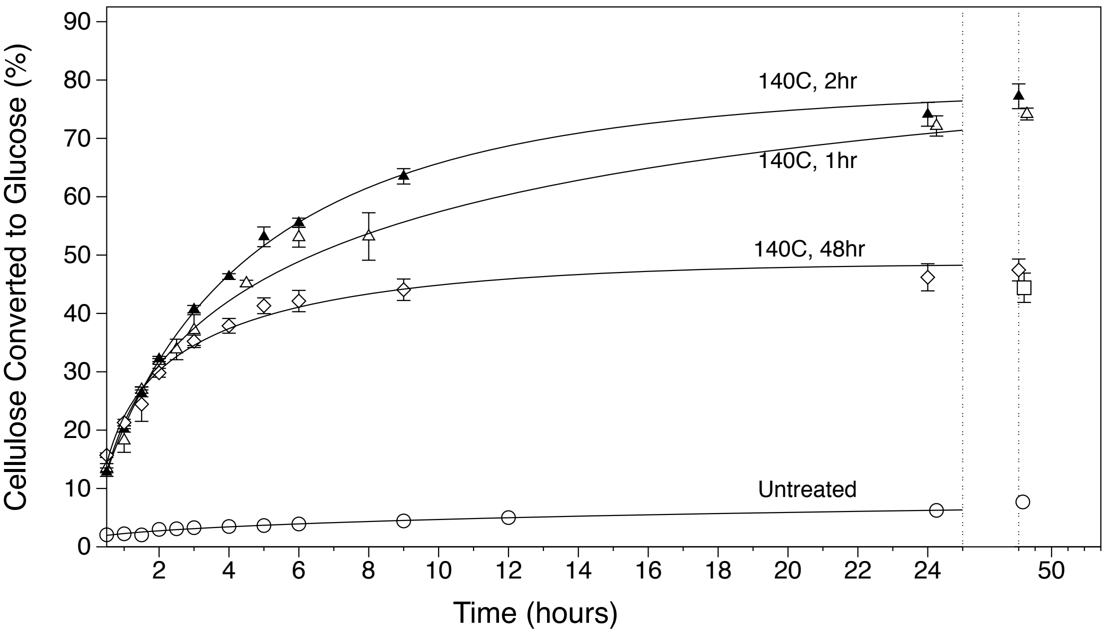

Figure A3. Enzymatic conversion of *Miscanthus* to glucose as a function of time. Ionic liquid pretreatment times were varied with a constant pretreatment temperature of 140°C. The enzymatic hydrolysis of untreated *Miscanthus* is shown for comparison.

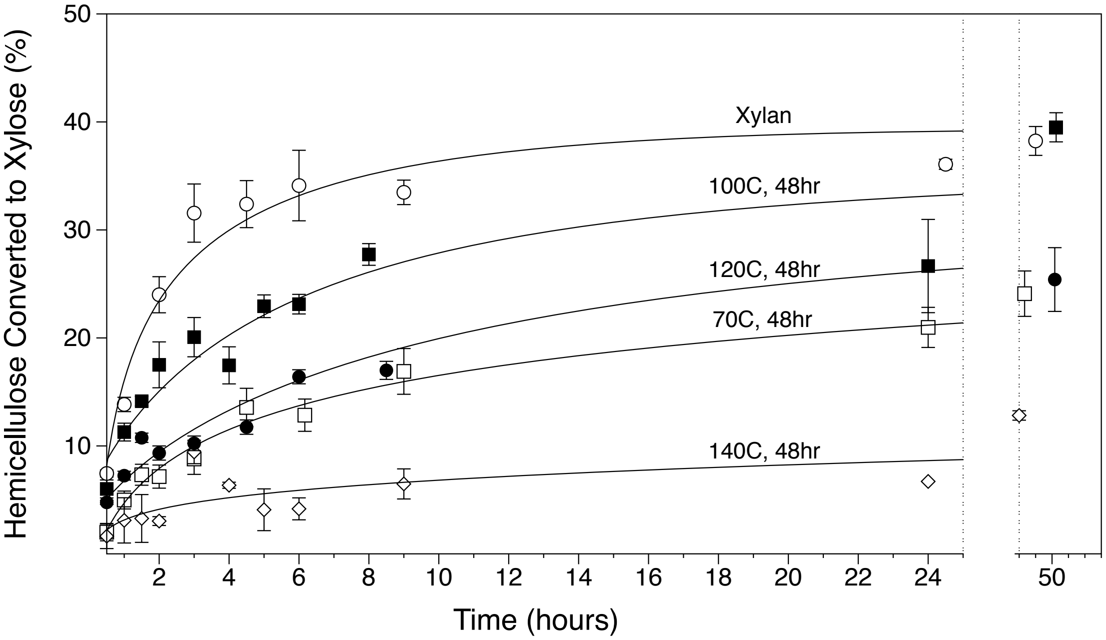

Figure A4. Enzymatic conversion of *Miscanthus* to xylose as a function of time. Ionic liquid pretreatment temperatures were varied with a constant pretreatment time of 48 h. The enzymatic hydrolysis of untreated xylan is shown for comparison.

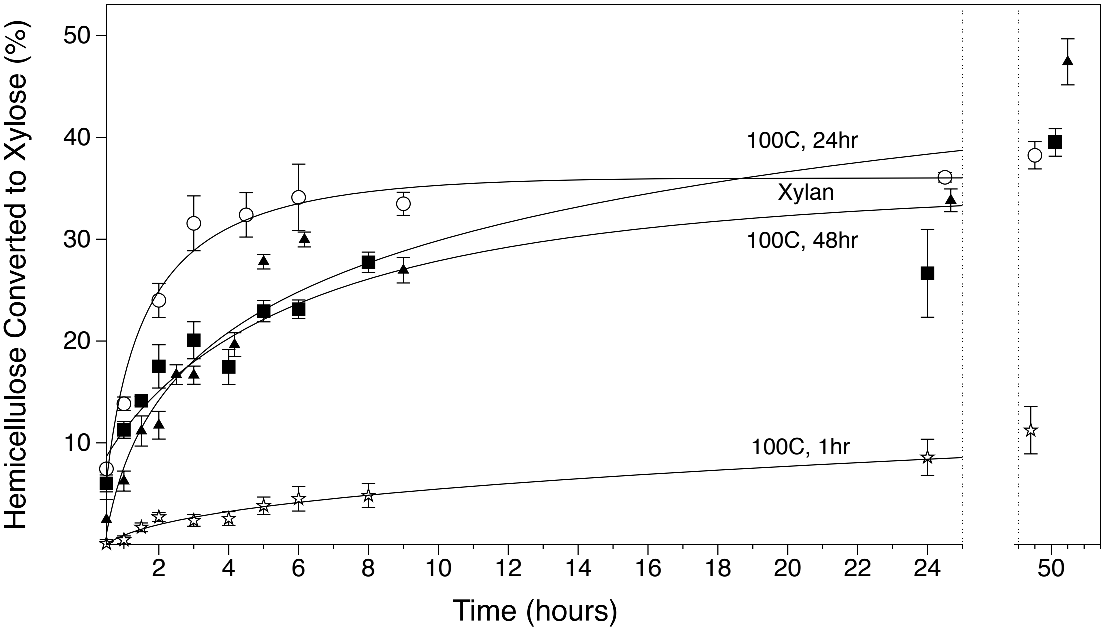

Figure A5. Enzymatic conversion of *Miscanthus* to xylose as a function of time. Ionic liquid pretreatment times were varied with a constant pretreatment temperature of 100°C. The enzymatic hydrolysis of untreated xylan is shown for comparison.

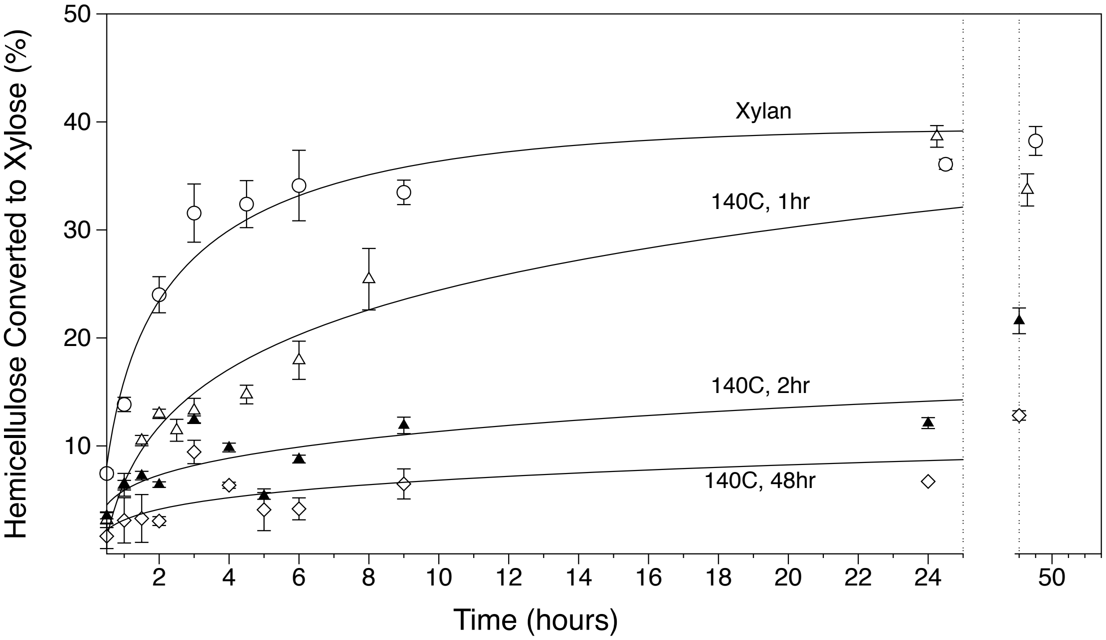

Figure A6. Enzymatic conversion of *Miscanthus* to xylose as a function of time. Ionic liquid pretreatment times were varied with a constant pretreatment temperature of 140°C. The enzymatic hydrolysis of untreated xylan is shown for comparison.

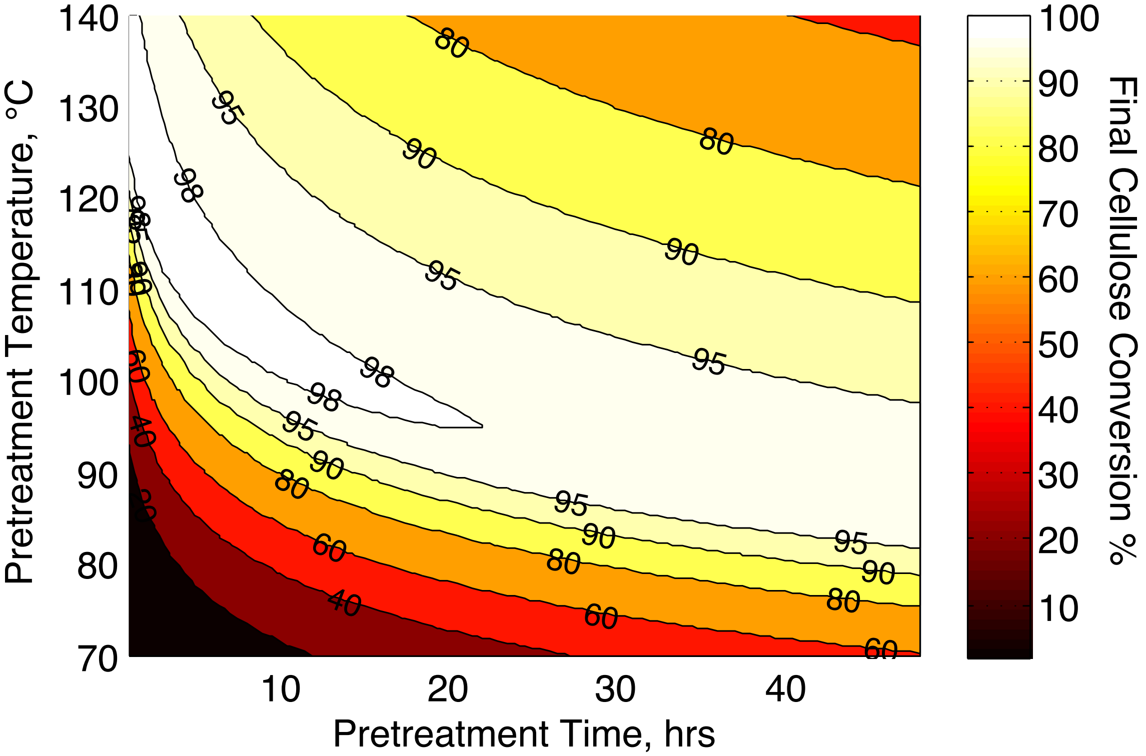

Figure A7. 2D contour plot of Arrhenius model fit of the final cellulose conversion vs pretreatment temperature and pretreatment time.

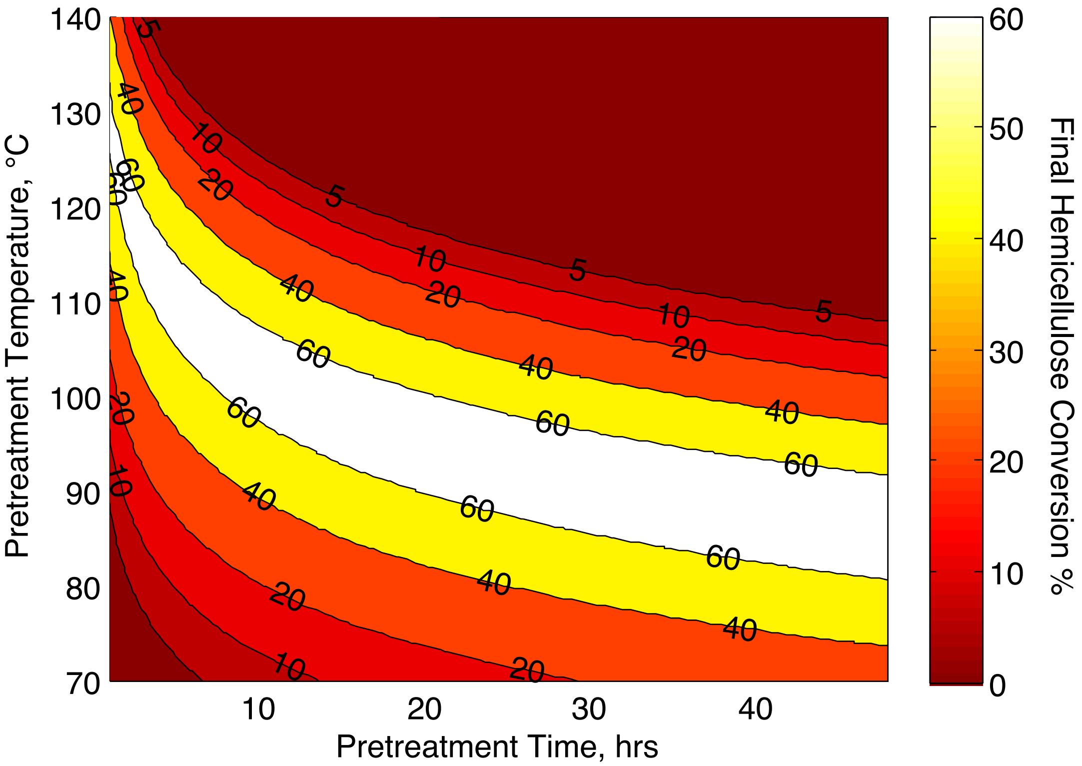

Figure A8. 2D contour plot of Arrhenius model fit of the final hemicellulose conversion vs pretreatment temperature and pretreatment time.

Calculation for energy to liberate a cellulose unit in Table 3.

For this rough comparison, we assume that the ionic liquid functions by decrystallizing the cellulose, liberating the surface edge glucan chains through breaking the H-bonds for each glucan unit. Gross and Chu (2010) show in Figure 4 (a) that a surface edge glucan unit has an average of 12.3 hydrogen bonds. Of these bonds, we assume two are intrachain O-H-O bonds, one is an interchain O-H-O bond, and the remaining are intersheet C-H-O bonds. Since dissolution does not break individual chains, we assume that the intrachain O-H-O bonds remain intact, which would leave 10.3 hydrogen bonds to break. One of these bonds would be the interchain O-H-O bond, with the remaining 9.3 bonds assumed to be C-H-O bonds. The interaction energies of the individual O-H-O bond and C-H-O bond are 6 kcal/mol and 2 kcal/mol, respectively (Gross and Chu, 2010). By summing the hydrogen bond energies for the one O-H-O bond and 9.3 C-H-O bonds, we find the energy to liberate one surface edge glucan unit to be 24.6 kcal/mol, or 1.0×10^5 J/mol.

Chapter 3

Glucose inhibition of cellulase enzymes following ionic liquid pretreatment of lignocellulosic biomass

Abstract

To meet the demands for biofuels production, a highly concentrated sugar product with minimal inhibitors is necessary for optimal fermentation conditions. However, at these high concentrations of sugars, product inhibition of cellulases and β-glucosidase can become a significant factor in the overall conversion of lignocellulose to glucose.

For this reason, we have studied enzymatic hydrolysis using a *Trichoderma reesei* cellulase cocktail supplemented with β-glucosidase from *Aspergillus niger* under varying glucose concentrations. We studied the production of cellobiose and glucose to understand how the product distribution changes over the course of hydrolysis. Avicel and 1-ethyl,3-methylimidazolium acetate ([Emim][OAc]) - pretreated Avicel were hydrolyzed to understand the effects of cellulose crystallinity on product inhibition. In addition, we used [Emim][OAc] - pretreated *Miscanthus* to understand the nature of the product profile on a realistic substrate with concentrations up to 25 g/L glucose.

We found glucose concentration to have a significant effect on the conversion of cellulose to glucose. For all reactions with initial glucose concentrations > 5 g/L, cellobiose accumulates during hydrolysis, peaking initially during the first 1.5 - 3 h of hydrolysis, and then slowly declining over the next 48 h. For higher glucose concentrations, a constant cellobiose concentration is present that does not decline over 48 h. The high concentrations of cellobiose found likely further inhibit the cellulases and the overall conversion as cellulose, even though the systems are supplemented with β-glucosidase. These effects are more pronounced with [Emim][OAc]-pretreated Avicel and *Miscanthus*.

Additionally, a competitive inhibition kinetic model was developed and fit to the enzymatic hydrolysis cellobiose and glucose profiles. The model was found to fit moderately well to the cellobiose and glucose hydrolysis data, but was unable to capture both the fast initial glucose production and constant cellobiose presence, highlighting the need for a more detailed mechanistic kinetic model.

1. Introduction

1.1 Economics of enzymatic hydrolysis

To meet the economic requirements for biofuels production from lignocellulosic biomass, a highly concentrated sugar solution (greater than 100 g/L glucose), containing minimal amounts of inhibitors, must be produced from biomass saccharification for optimal fermentation to fuels (Andrić et al., 2010c). In addition, the high cost of cellulase enzymes further demands operating at high conversions to produce the concentrated sugar product (Klein-Marcuschamer et al., 2011). Enzymatic hydrolysis can be performed at low biomass loadings to produce less concentrated sugar streams, which can then be concentrated through membrane technology (Andrić et al., 2010b; Gan et al., 2002). This process is still being developed but may be costly due to high reactor volume requirements and membrane costs (Andrić et al., 2010b; Jørgensen et al., 2007). The ideal, economical way to produce a concentrated sugar solution is to operate at a high solids loading with high conversions. This has been studied in detail by improving reactor and process design (Gusakov et al., 1987), as well as by use of various enzyme recycle schemes . However, operating at high solids loading typically results in low biomass conversion to sugars. This is often attributed to buildup of lignin and un-hydrolyzed material, and mixing/viscosity effects. In addition, another complex issue is the nature of enzymatic hydrolysis in a highly concentrated sugar environment.

1.2 Product inhibition of cellulases

The hydrolysis of cellulose is complex, requiring a mixture of cellulases for optimal conversion to glucose. Cellulases produce cellobiose as their primary product (Holtzapple et al., 1990; Levinson et al., 1951); however, cellobiose can be inhibitory to further conversion of cellulose to cellobiose (Andrić et al., 2010c; Holtzapple et al., 1990; Katz and Reese, 1968; Oh et al., 2000; Reese et al., 1952). While the mechanism of cellobiose inhibition is not well understood, it inhibits both endoglucanases and exoglucanases of *Trichoderma reesei* (Andrić et al., 2010c; Dekker, 1986; Gruno et al., 2004; Holtzapple et al., 1990; Murphy et al., 2013). However, the mechanism and kinetics of inhibition can vary greatly depending on the experimental parameters. The type and purity of the enzyme, type of substrate (soluble or insoluble), and measurement method all influence the kinetics of the system (Andrić et al., 2010c; Gruno et al., 2004; Gusakov and Sinitsyn, 1992; Holtzapple et al., 1990). Due to the heterogeneous nature of cellulose catalysis, a simple Michaelis-Menten model rarely describes the system behavior (Andrić et al., 2010c; Holtzapple et al., 1990).

In addition, the mechanism of product inhibition is unclear, with a variety of studies reporting competitive, non-competitive, or mixed mechanisms and a variety of inhibition constants (Andrić et al., 2010c; Holtzapple et al., 1990). As a result, there is a wide range of reported K_I's for cellulases from *T. reesei* (Andrić et al., 2010c). In addition to kinetic parameters, Murphy et al. represented the inhibition by reporting the inhibitor concentration at which the enzyme activity is reduced by 75% (Murphy et al., 2013). This representation provides a better idea about what concentrations of cellobiose are tolerated during hydrolysis, and shows the full impact on activity at these relatively low inhibitor concentrations (Andrić et al., 2010c; Murphy et al., 2013). A summary of the inhibition kinetics and mechanisms from the literature is provided in Table 1.

Due to cellobiose inhibition of cellulases, β-glucosidase is often added to convert cellobiose to glucose and is necessary to achieve high conversions of cellulose to glucose (Andrić et al., 2010c; Katz and Reese, 1968; Sternberg et al., 1977). Glucose is less inhibitory than cellobiose (Andrić et al., 2010c; Katz and Reese, 1968). Glucose inhibition of cellulases is complex and not fully understood, and the literature shows a wide range of K_I's and mechanisms for this phenomenon (See Table 1) (Andrić et al., 2010c; Murphy et al., 2013). While cellobiose is generally thought to be more inhibitory than glucose for cellulases, Murphy et al. found that for cellobiohydrolase II from *Trichoderma reesei*, glucose is actually more inhibitory than cellobiose, showing that the addition of β-glucosidase is not necessarily beneficial (Andrić et al., 2010c; Murphy et al., 2013). However, the addition of β-glucosidase has been shown in many studies to greatly improve the hydrolysis of solid cellulose substrates by the cellulase cocktail (Kadam et al., 2004; Sternberg et al., 1977).

1.3 Product inhibition of β-glucosidase

What additionally complicates this system is that β-glucosidase has been shown to be product inhibited. β -glucosidase is inhibited by glucose, which then slows the conversion of cellobiose to glucose (Andrić et al., 2010c; Dekker, 1986; Oh et al., 2000; Xiao et al., 2004). This buildup of both glucose and cellobiose can thus further inhibit the system, causing significant product inhibition, as illustrated in Figure 1. While β-glucosidase acts on soluble substrates, the nature of its product inhibition is elusive (Andrić et al., 2010c; Bohlin et al., 2010; Chauve et al., 2010). A variety of types of inhibition have been attributed to β-glucosidase, and its inhibition kinetic constants have a wide range of values (Table 1), often depending on enzyme purity and whether the substrate is cellobiose or a fluorescent substitute (Andrić et al., 2010c; Bohlin et al., 2010). Additional complications have been described at high cellobiose loadings, where substrate inhibition and the conversion of cellobiose into oligosaccharides can occur (Andrić et al., 2010a; Andrić et al., 2010c; Chauve et al., 2010; Watanabe et al., 1992).

Cellulases from *Trichoderma reesei*		**β-Glucosidase from *Aspergillus niger***	
Cellobiose inhibition		Cellobiose inhibition	
K_I	0.01 - 34 mM	K_I	50 mM
IC_{75}	2 g/L (CBHI)		Effects > 4 g/L
Proposed mechanisms	Competitive, noncompetitive, mixed	Proposed mechanisms	Substrate
Glucose inhibition		Glucose inhibition	
K_I	10 – 30 mM	K_I	0.2 – 14 mM
IC_{75}	3 g/L (CBHII)	IC_{75}	6 g/L*
Proposed mechanisms	Competitive, noncompetitive, mixed	Proposed mechanisms	Competitive, noncompetitive, uncompetitive, mixed

*From this work, Novo188 activity at 50°C after 10min hydrolysis of 1wt% cellobiose solution.

Table 1. The range of inhibition constants from the literature for cellulases from *Trichoderma reesei* and β-glucosidase from *Aspergillus niger* (Andrić et al., 2010c; Bohlin et al., 2010; Calsavara et al., 1999; Chauve et al., 2010; Dekker, 1986; Gruno et al., 2004; Jørgensen et al., 2007; Levine et al., 2010; Murphy et al., 2013).

1.4 Modeling efforts for enzymatic hydrolysis

This complicated system of multiple enzymes with feedback inhibition makes the optimization and modeling of a full enzyme mixture on a lignocellulosic substrate daunting (Andrić et al., 2010a; Holtzapple et al., 1990). Many groups have tackled the modeling of both β-glucosidase and cellulases, from individual enzymes to the whole mixture on lignocellulosic substrates (Andrić et al., 2010a; Bansal et al., 2009; Chauve et al., 2010; Gan et al., 2003; Gruno et al., 2004; Gusakov et al., 1985; Holtzapple et al., 1990; Kadam et al., 2004; Khodaverdi et al., 2011; Levine et al., 2010; Zheng et al., 2009). Model substrates and purified enzymes are often used not only to obtain detailed and accurate kinetics, but also to simplify the system (Andrić et al., 2010c). However, these simplifications do not necessarily translate to a complete enzyme mixture acting on a pretreated lignocellulosic substrate (Andrić et al., 2010a; Andrić et al., 2010c; Wald et al., 1984). In addition, inhibition and kinetic data are often only collected for initial rates and final conversions, and rarely is the full product time profile presented. However, these time profiles can provide valuable data not only for process engineering optimization, but also gives an insight into the transient nature of enzymatic hydrolysis.

For this reason, we have studied the enzymatic hydrolysis of ionic liquid (IL) pretreated *Miscanthus* with a *Trichoderma reesei* cellulase cocktail, supplemented with β-glucosidase from *Aspergillus niger* under varying glucose concentrations. We collected the time-resolved production of cellobiose and glucose to understand how the product distribution changes over the course of hydrolysis and glucose concentration. We studied Avicel and 1-ethyl, 3-methylimidazolium acetate, [Emim][OAc], pretreated Avicel to understand the effects of cellulose crystallinity on product inhibition and the hydrolysis profile. In addition, we used [Emim][OAc}-pretreated *Miscanthus* to examine the product profile with concentrations up to 25 g/L glucose.

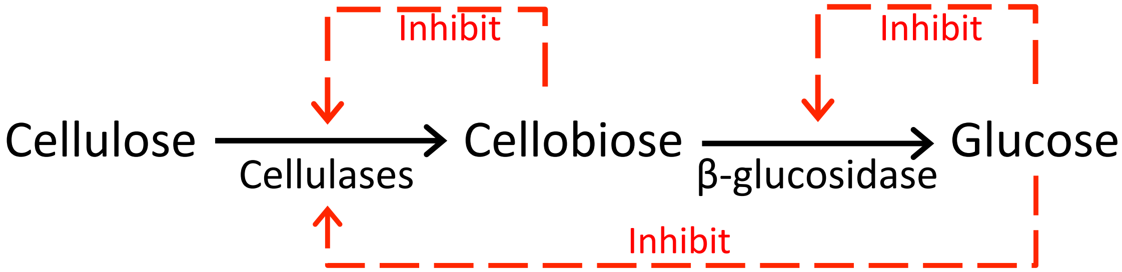

Figure 1. Simplified reaction scheme for the conversion of cellulose to glucose and the inhibition pathways.

2. Materials and Methods

2.1 Materials

Substrates. D-(+)-glucose was purchased from Sigma Aldrich (G8270-10KG). Avicel PH-101 (11365-1KG) and D-(+)-cellobiose (22150-10g) were purchased from Fluka. *Miscanthus x giganteus* was provided by the University of Illinois, Urbana-Champaign and was ground through a 4 mm sieve plate, resulting in a heterogeneous mixture of particles up to 1 cm.

Enzymes. Enzymes used were commercial mixtures purchased from Sigma Aldrich. The β-glucosidase from *Aspergillus niger* (Novo188, Product # C6105-50ML) and cellulase cocktail from *Trichoderma reesei* (Celluclast 1.5L, Product # C2730-50ML) were used without further purification. The activity of Novo188 was reported to be 279 CBU/g, and the protein concentration measured as 28.8 mg protein/mL by Bradford assay (Bio-Rad). In addition, the sugar concentration of the enzyme preparation was measured with HPLC, and contained 146 g/L glucose and 60.6 g/L cellobiose. The Celluclast's activity was reported to be 790 units/g, and a filter paper assay was performed with the activity measured to be 118 FPU/mL (Ghose, 1987). The protein concentration of the Celluclast was 43.4 mg protein/mL by Bradford assay (Bio-Rad).

Chemicals. Citrate buffer was produced from citric acid (C2404-500G) and sodium citrate tribasic dihydrate (C8532-500G) purchased from Sigma Aldrich. IL pretreatment was performed with 1-ethyl-3-methylimidazolium acetate from Iolitec (IL-0189-TG-0500, >95% pure).

2.2 Pretreatment

For the pretreatment of Avicel, [Emim][OAc] was preheated to 100°C with stirring in a silicone oil bath. Once to temperature, Avicel was added to a 10 wt% solution. The solution was stirred at 100°C for 1 h to ensure Avicel dissolution. After 1 h, the solution was cooled to 80°C and nanopure water at 80°C was slowly added in a 1:1 volume ratio to precipitate the cellulose. The mixture was separated by centrifugation at 5000 rpm for 5 min. The supernatant was removed, and the solids re-suspended in citrate buffer and the mixture centrifuged. This process was repeated until the pH of the solution was 4.8 and optically clear. The solution was stored in buffer until enzymatic hydrolysis.

For the pretreatment of *Miscanthus*, [Emim][OAc] was preheated to 100°C with stirring in a silicone oil bath. Once to temperature, *Miscanthus* was added to make a 5 wt% solution (total biomass). The solution was stirred at 100°C for 48 h to ensure dissolution and to make a very easily enzymatically hydrolysable substrate (Shill et al., 2012). After 48 h, the solution was cooled to 80°C and nanopure water at 80°C was slowly added in a 1:1 volume ratio to precipitate the cellulose. The mixture was then washed in the same fashion as the Avicel and stored in buffer until further use.

2.3 Enzymatic hydrolysis

Enzymatic hydrolysis occurred at a 1 wt% cellulose (~2 wt% biomass for *Miscanthus*) loading in citrate buffer (pH 4.8, 50 mM), with 0-16 g/L initial glucose concentrations. A 125 mL Erlenmeyer flask was filled with 50 g total solution (biomass, starting glucose and buffer) and 200 μL of 5% v/v sodium azide solution to prevent microbial contamination (Selig et al., 2008). The reactors were heated to 50°C while stirring overnight to ensure glucose dissolution and isomerization. One-mL samples were taken before hydrolysis to get baseline glucose readings. To begin hydrolysis, 0.0625 mL each of Celluclast and Novo188 was added to the solution. Unless otherwise stated, 1 mL samples were withdrawn at designated time intervals and immediately added to 70.5 μL of 1 M KOH to bring the pH to 8.6. Then the solutions were quickly frozen with dry ice and stored until further analysis. These steps were taken to quickly stop the reaction and ensure upon thawing and analysis that further hydrolysis was unlikely. The reactors were run in duplicate, and all errors represent the standard error between samples taken from these reactors.

2.4 Analysis

Glucose and cellobiose concentrations were determined by high performance liquid chromatograph (Shimadzu). Samples were analyzed with an RFQ Fast Acid Column (Phenomenex Inc.) at 55°C using 0.01 N sulfuric acid pumped at 1 mL/min as the mobile phase.

2.5 Competitive inhibition modeling

To study the product inhibition of enzymatic hydrolysis, a basic Michaelis-Menten kinetic model with competitive inhibition was implemented. The cellulase kinetics were lumped into a single reaction scheme where the enzymes bind reversibly to cellulose, and then irreversibly create the cellobiose product, following pseudo-steady state Michaelis Menten kinetics (Briggs and Haldane, 1925; Michaelis and Menten, 1913). A similar model was applied for the β-glucosidase catalysis of cellobiose to glucose. Competitive inhibition was modeled assuming equilibrium conditions, with cellobiose inhibiting the cellulases, and glucose inhibiting both cellulase and β-glucosidase activity. The reaction scheme and full derivation are shown in the Appendix.

Initial cellulose $[S]_0$, glucose $[G]_0$, cellulase $[E_c]_0$, and β-glucosidase $[E_\beta]_0$ concentrations were constants. An Excel spreadsheet with increasing time steps of 30 s was made, where at each time point the cellulose [S], cellobiose [C], and glucose [G] concentrations were calculated from the change in cellobiose d[C]/dt and glucose d[G]/dt using the earlier product concentrations and calculated enzyme-substrate concentrations. These equations, constants, and variables are shown in the Appendix. Initial guesses were made for the kinetic parameters (K_{mc}, k_{catc}, $K_{m\beta}$, $k_{cat\beta}$, K_{cIC}, K_{cIG}, and $K_{\beta IG}$) based on literature values (Table 3). The 2011 Excel Solver package from Frontline Systems was used to determine the best fit for the 7 variables by maximizing the correlation coefficients for both cellobiose and glucose simultaneously.

3. Results and Discussion

3.1 Glucose inhibition during the hydrolysis of untreated Avicel

The effect of glucose on the enzymatic conversion of a crystalline substrate to cellobiose and glucose was studied using untreated Avicel. Figure 2 shows the concentration profiles of cellobiose and glucose at various initial glucose concentrations. Peak and final concentrations are shown in Table 2. The results show that glucose produced by the enzymes decreases with increasing glucose concentration. In addition, the total conversion of Avicel to glucose and cellobiose decreases with increasing glucose present. In the scenario with no initial glucose, there is no detectable cellobiose present during the entire time course of the hydrolysis. However, when glucose is added before hydrolysis, cellobiose accumulates and increases during the first 1.5 h of hydrolysis, and then slowly declines over the next 48 h. For the scenario with 5.62 g/L glucose initially present, the cellobiose is no longer detectable after 24 h. However, for the higher glucose concentrations, a constant cellobiose concentration is present that does not decline over 48 h (reactions were carried out to 100 h and cellobiose was still present at similar concentrations).

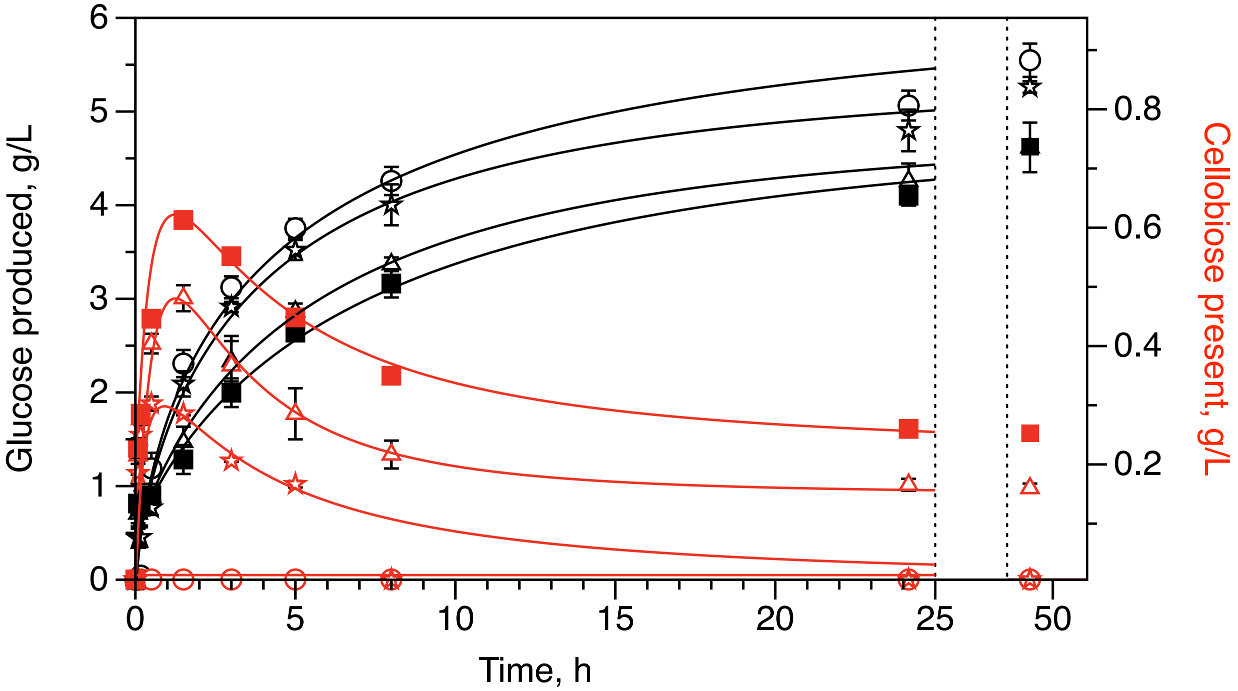

Figure 2. The enzymatic conversion of Avicel to cellobiose (red) and glucose (black) with varying initial glucose concentrations (○ - 0g/L, ☆ – 5.62 g/L, △ – 11.1 g/L, ■ - 16.2 g/L). Error bars represent one standard deviation.

3.2 Glucose inhibition during the hydrolysis of [Emim][OAc]-pretreated Avicel

For the [Emim][OAc]-pretreated Avicel studies, we wanted to determine the differences in the product evolution of glucose and cellobiose from an amorphous substrate as compared to the highly crystalline Avicel. Figure 3 shows the time course of cellobiose and glucose generation with various initial glucose concentrations. Peak and final concentrations are also shown in Table 2. For all scenarios, cellobiose was initially formed and then its concentration gradually decreased.

In the reaction without any initial glucose, the cellobiose concentration peaked at 0.83 g/L after 1.5 h, and then declined to an undetectable concentration after 24 h. This is in contrast to the hydrolysis with untreated Avicel, where cellobiose was not detected at all during the hydrolysis in the absence of initial glucose. This suggests that the cellulases produce cellobiose more rapidly than it can be converted to glucose by β-glucosidase. This may be due to the fact that [Emim][OAc]-pretreated Avicel is much more easily hydrolyzed than crystalline Avicel, which increases the rate of cellobiose production by the cellulases. Since the cellobiose substrate is the same for the β-glucosidase, the β-glucosidase rate remains unchanged while the cellulase rate is higher, causing a buildup of cellobiose. Another explanation could be that the hydrolysis of [Emim][OAc]-pretreated Avicel proceeds so quickly that glucose is produced at a very fast rate (with concentrations exceeding 5 g/L within the first 1.5 h), which may additionally inhibit the β-glucosidase, resulting in cellobiose accumulation.

For the reactions with initial glucose present, an increase in cellobiose concentration occurs, followed by a gradual decrease to a constant, low cellobiose concentration that does not decline after 48 h. In the case of 15.7 g/L glucose initially present, cellobiose increases to a concentration of 2.48 g/L at 1.5 h, and then declines to 0.33 g/L. These high initial cellobiose concentrations in the hydrolysis may have quite a strong inhibitory effect on cellulase activity (Murphy et al., 2013), thus slowing down the overall conversion.

The trend of an initial increase and gradual decline in cellobiose concentration has been previously reported by Khodaverdi et al. on NMMO-pretreated cotton linter, which should be similar in behavior to [Emim][OAc]-pretreated Avicel because of its decrystallized nature (Khodaverdi et al., 2011). In addition, the model proposed by Khodaverdi predicted inhibition constants that were higher for NMMO treated cotton linter as compared to untreated cotton linter (Khodaverdi et al., 2011).

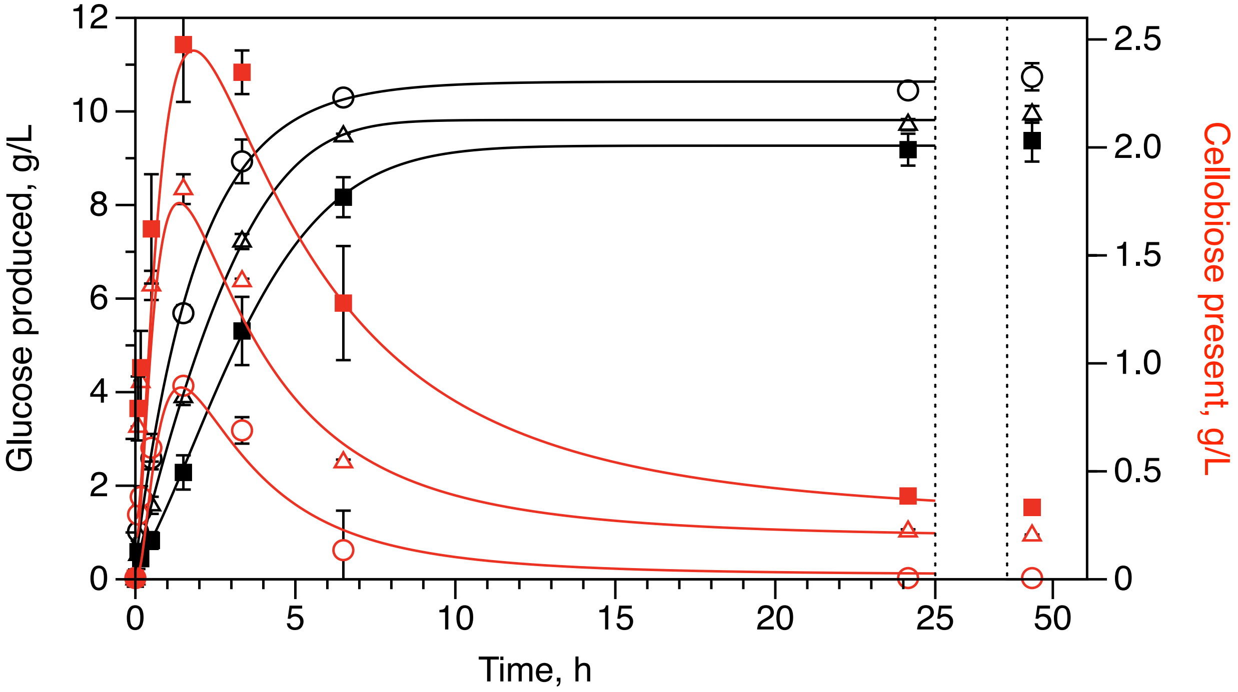

Figure 3. The enzymatic conversion of [Emim][OAc]-pretreated Avicel to cellobiose (red) and glucose (black) with varying initial glucose concentrations (○ - 0g/L, △ – 7.36 g/L, ■ - 15.7 g/L). Error bars represent one standard deviation.

3.3 Glucose inhibition of [Emim][OAc]-pretreated Miscanthus

For the [Emim][OAc]-pretreated *Miscanthus* studies, we wanted to determine how hydrolysis of pretreated biomass was affected by the presence of glucose, and the roles of hemicellulose and lignin on reaction rates. Hemicellulose and lignin can potentially inhibit cellulases by acting as competitive, unproductive binding substrates.

Figure 4 shows the time course of cellobiose and glucose evolution at various initial glucose concentrations. Peak and final concentrations are also shown in Table 2. Similar time courses to those of the [Emim][OAc]-pretreated Avicel were observed. The scenario with no initial glucose had a small but measurable cellobiose concentration at 1.5 h that quickly declined.

For the reactions with initial glucose present, an increase in cellobiose concentration occurred. This gradually decreased to a constant, low cellobiose concentration that did not decline after 48 h. In the case with 16.1 g/L glucose initially present, cellobiose increased to a concentration of 1.82 g/L at 3 h, and then declined to 0.79 g/L. A noticeable difference in this case is that the maximum cellobiose concentration is attained at a later time than the [Emim][OAc]-pretreated Avicel, and while a high concentration was obtained, it is not as high as that from [Emim][OAc]-pretreated Avicel. This may be due to the slower reaction rate on this lignocellulosic substrate, decreasing the rate of production of cellobiose and glucose.

Another interesting characteristic from the hydrolysis of [Emim][OAc]-pretreated *Miscanthus* is the shape of the cellobiose time courses. The presence of elevated cellobiose concentrations is more prolonged over the 48 h period and does not decrease as rapidly as with the [Emim][OAc]-pretreated Avicel. The final concentration of cellobiose is also much higher than [Emim][OAc]-pretreated Avicel, indicating a much more inhibited system. This could be due to the competitive and unproductive binding from the lignin and hemicellulose (Andrić et al., 2010c). It could also be due to the presence of other inhibitors, such as xylose (Kadam et al., 2004; Xiao et al., 2004). Similarly shaped production curves have been shown in the literature on other lignocellulosic substrates at high solids loadings (Kadam et al., 2004; Wald et al., 1984).

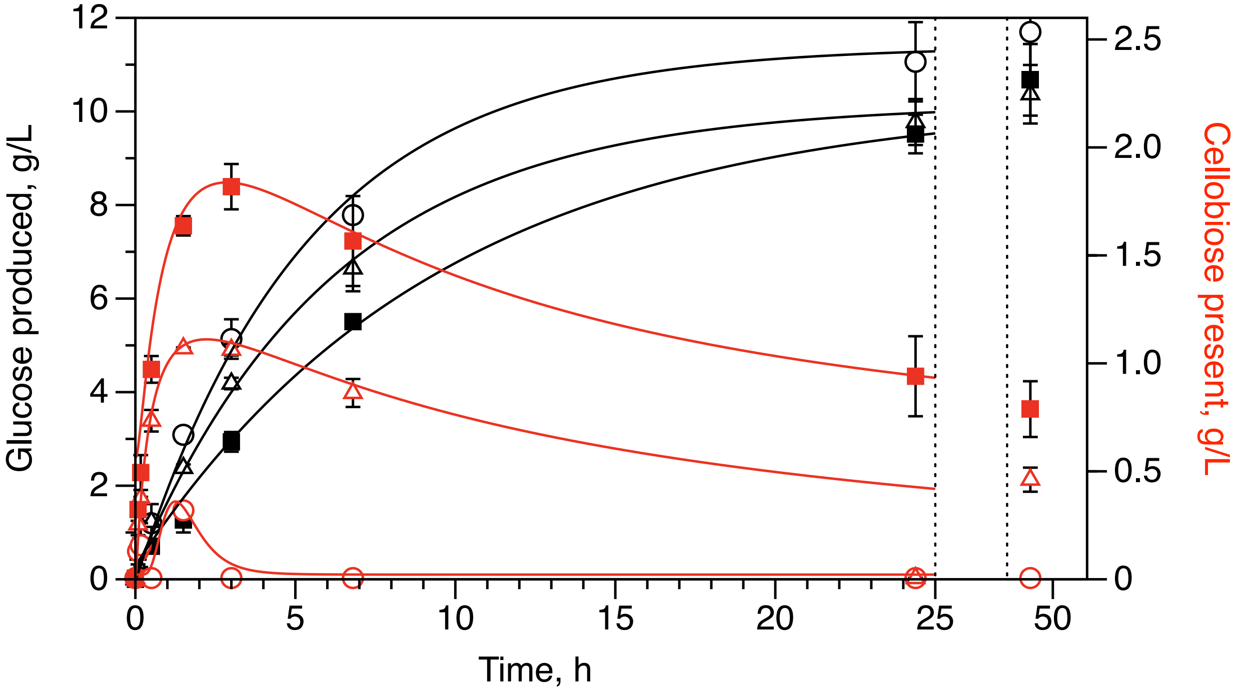

Figure 4. The enzymatic conversion of [Emim][OAc]-pretreated *Miscanthus* to cellobiose (red) and glucose (black) with varying initial glucose concentrations (○ - 0g/L, △ – 7.53 g/L, ■ - 16.1 g/L). Error bars represent one standard deviation.

		Max cellobiose concentration reached			**Final conditions**		
	Initial glucose conc (g/L)	**Time (h)**	**Cellobiose (g/L)**	**Total glucose (g/L)**	**Time (h)**	**Cellobiose (g/L)**	**Total glucose (g/L)**
Avicel	0 ± 0	NA	NA	NA	100.3	0.0 ± 0.0	6.32 ± 0.14
	5.62 ± 0.08	0.5	0.30 ± 0.01	6.38 ± 0.08	100.3	0.0 ± 0.0	11.1 ± 0.29
	11.1 ± 0.11	1.5	0.48 ± 0.02	12.5 ± 0.16	100.3	0.17 ± 0.03	16.0 ± 0.44
	16.2 ± 0.10	1.5	0.61 ± 0.00	17.5 ± 0.15	100.3	0.27 ± 0.00	21.1 ± 0.01
[Emim][OAc] Avicel	0.0 ± 0.0	1.5	0.83 ± 0.03	5.69 ± 0.17	48.2	0.0 ± 0.0	10.7 ± 0.29
	7.36 ± 0.21	1.5	1.81 ± 0.07	11.3 ± 0.17	48.2	0.20 ± 0.00	17.3 ± 0.18
	15.7 ± 0.11	1.5	2.48 ± 0.27	18.0 ± 0.37	48.2	0.33 ± 0.01	25.1 ± 0.44
[Emim][OAc] *Miscanthus*	0.0 ± 0.0	1.5	0.32 ± 0.02	3.09 ± 0.13	48.0	0.0 ± 0.0	11.7 ± 1.09
	7.53 ± 0.02	1.5	1.07 ± 0.00	9.91 ± 0.07	48.0	0.46 ± 0.06	17.9 ± 0.63
	16.1 ± 0.09	3.0	1.82 ± 0.10	19.1 ± 0.21	48.0	0.79 ± 0.13	26.8 ± 0.77

Table 2. Results for the hydrolysis of Avicel, [Emim][OAc] – pretreated Avicel, and [Emim][OAc] – pretreated *Miscanthus* at varying initial glucose concentrations. Error represents one standard deviation.

3.4 The role of β-glucosidase

To better understand the inhibition of β-glucosidase, several studies with only Novo188 were performed. First, Novo188 was subjected to various stressors to determine whether activity was lost during the course of hydrolysis. This experiment was to see if Novo188 activity loss was the cause of the long-term cellobiose presence found in the hydrolysis time-courses on biomass.

To determine whether temperature and shaking were deactivating Novo188, 0.0625mL of Novo88 was placed in a reactor with 50 g of 1 wt% cellobiose solution in citrate buffer at 50°C. After 10 min, the glucose concentration was measured by a YSI Biochemistry Analyzer 2700 Select equipped with a glucose membrane. This was compared to an incubation study where Novo188 was placed in the citrate buffer at 50°C and was left to shake for 72 h. After 72 h, cellobiose was added to make a 1 wt% solution, and the glucose produced was measured after 10 min. Reactors were run in duplicate. To determine whether Avicel presence had an effect on Novo188 stability, the same experiment was performed as for temperature/shaking, with the addition of a 1 wt% Avicel concentration to the reactors. All other conditions were identical. To determine whether glucose presence affected Novo188 stability, the same experiment was performed as with Avicel, but with the addition of 14.8 g/L glucose concentration to the reactors. Activity was measured by first measuring the glucose concentration by YSI before the addition of Novo188 and then measuring glucose produced after 10 min of hydrolysis. The results in Figure 5 show that, within error, there was no loss in activity over 72 h due to temperature incubation, shaking, Avicel, or glucose presence. While there is a decrease in activity due to glucose presence, this is an inhibitory effect, and there is no activity loss due to the incubation of Novo188 with glucose.

Additional studies were performed where only cellobiose, glucose, and β-glucosidase were present. A reactor with the same concentration of β-glucosidase was charged with the final cellobiose and glucose concentrations attained in the 16.2 g/L glucose reaction from Figure 2. The results are shown in the Appendix in Figure A1, and support the finding of a sustained cellobiose concentration resulting from severe inhibition of β-glucosidase at high glucose, low cellobiose loadings.

The role of β-glucosidase concentration was also studied. The 16.2 g/L glucose case on Avicel, shown in Figure 2, was replicated with 10x the Novo188 concentration. To avoid interference from the Novo188 native sugar concentration, the solution was first run through a GE PD-10 desalting column to remove the sugars before addition to the hydrolysis reactor. The time-course hydrolysis profile is shown in the Appendix in Figure A2, and shows a similar stabilization of the cellobiose concentration. The initial peak in cellobiose concentration is less than that found with the original β-glucosidase concentration, but the reactor attains similar final glucose and cellobiose concentrations. Additionally, with the protein loading of β-glucosidase being ~4 wt% of the cellulose, this is an impractical and cost-prohibitive hydrolysis scenario for industrial-scale biofuel production.

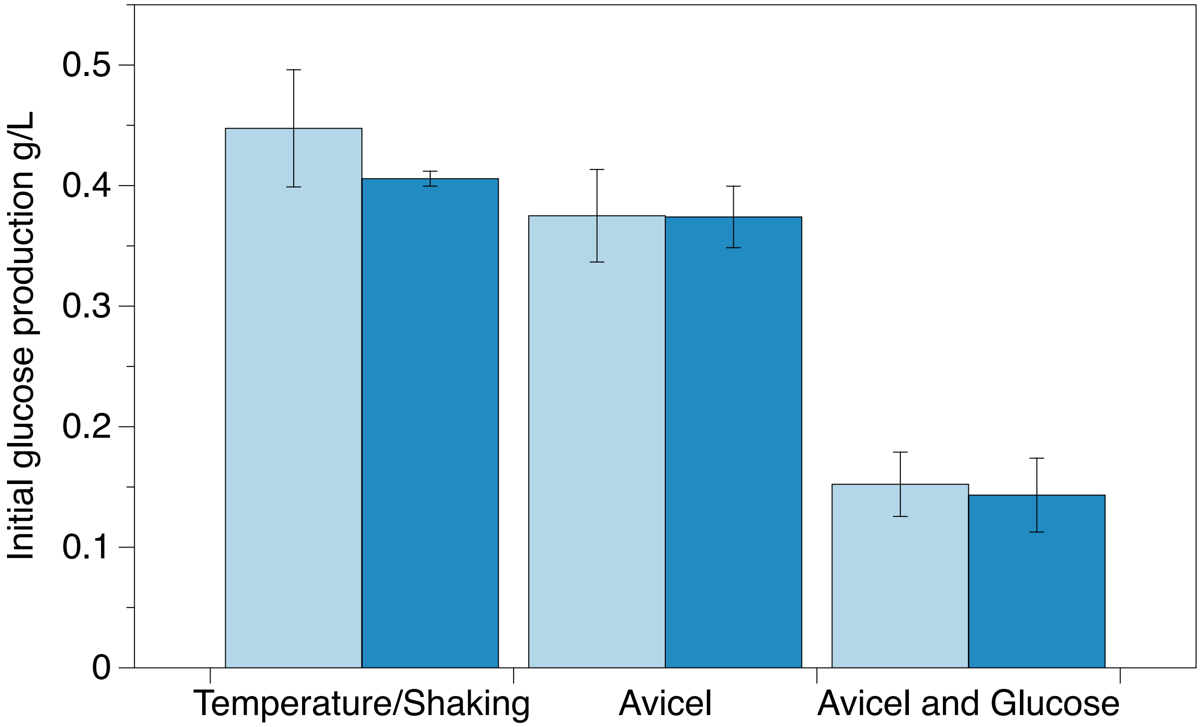

Figure 5. The initial glucose production from the hydrolysis of cellobiose by β-glucosidase under various processing stressors (light blue – initial production, dark blue, initial production after 72 h incubation). Error bars represent one standard deviation.

3.5 Competitive inhibition modeling

The competitive inhibition model described in the Methods section was fit to the 16.1 g/L initial glucose hydrolysis of [Emim][OAc]-pretreated *Miscanthus*, and the results are shown in Figure 6. The solution with the best fit for both cellobiose and glucose is shown, with an R^2 of 0.87 for the glucose data and R^2 of 0.88 for the cellobiose data. While the model fits reasonably well for such a complicated hydrolysis scenario, it is not able to characterize the initial rate of glucose production combined with the high concentration of cellobiose at long hydrolysis times. If, for example, we only fit the model to the glucose data, an R^2 of 0.98 can be achieved (see Figure A3 (a)). However, this solution does not predict the cellobiose curve well, resulting in an R^2 of 0.48. This analysis can be similarly performed for fitting the model only to the cellobiose curve, which results in a poor fit of the glucose data (see Figure A3 (b)). This analysis shows the importance of monitoring both glucose and cellobiose over the course of enzymatic hydrolysis, especially when developing a model to solve for kinetic parameters.

The kinetic parameters resulting in the best fit of both the cellobiose and glucose data are shown in Table 3. Additionally, a sensitivity analysis was performed and showed that the parameters that most affect the quality of the fit are the cellulase K_m and, unsurprisingly, the K_m, K_i, and k_{cat} of the β-glucosidase.

Additionally, this model was used to fit the Avicel and [Emim][OAc]-pretreated Avicel, as well as the [Emim][OAc]- pretreated *Miscanthus* at lower initial glucose concentrations. Similar behavior of the model was found regardless of substrate or inhibitor concentration. The inability of the model to fit the initial rate of glucose production combined with high cellobiose concentration indicates that there is something fundamentally lacking in the model to describe this behavior.

Very few models in the literature have attempted to fit a model to both cellobiose and glucose hydrolysis profiles from lignocellulose. Kadam et al. used a very similar competitive inhibition model, but with the addition of a parameter that represented the digestibility of the substrate (Kadam et al., 2004). Wald et al. also modeled the hydrolysis of lignocellulose with some success, yet a closer look at their model shows that they are also unable to predict the sustained cellobiose concentrations seen over time (Wald et al., 1984). A more mechanistic model, accounting for the multiple enzyme kinetics from different cellulases and the nature of the cellulosic substrate, may be more appropriate and provide a better fit and insight into the inhibition kinetics (Levine et al., 2010; Levine et al., 2011).

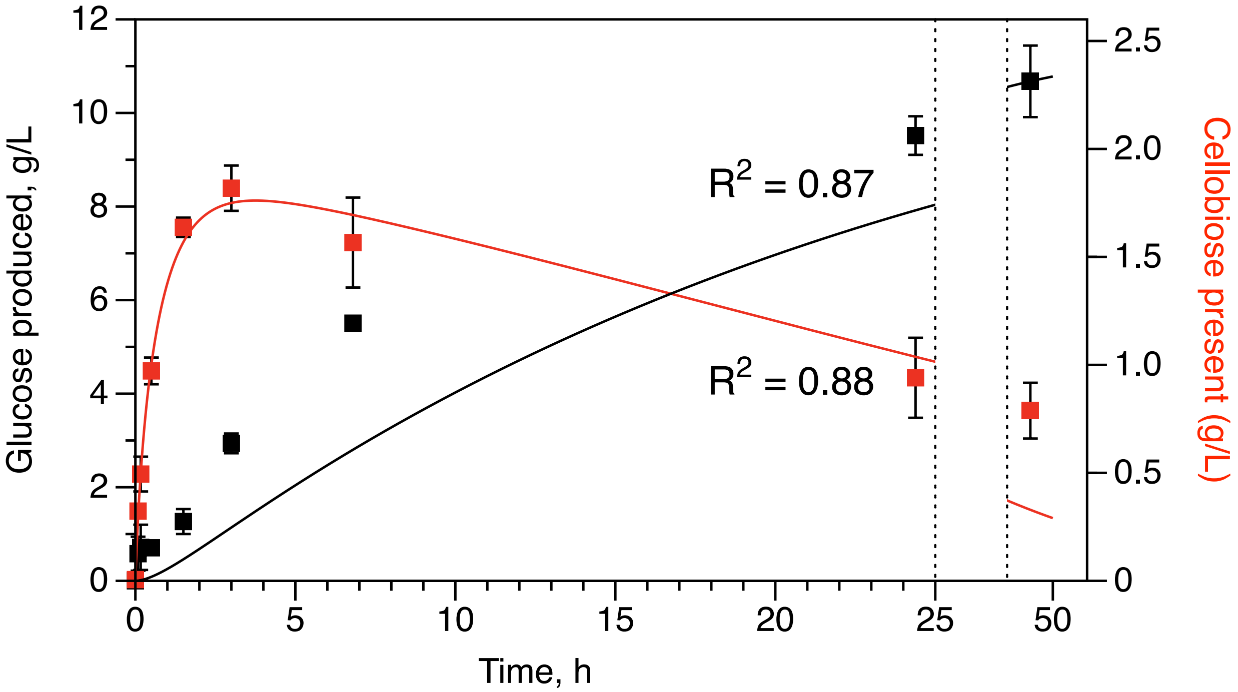

Figure 6. Model for the enzymatic conversion of [Emim][OAc]-pretreated *Miscanthus* to cellobiose (red) and glucose (black) with 16.1 g/L initial glucose concentration. The lines represent the model's predicted cellobiose and glucose concentrations.

Kinetic constants	**Initial guess**	**Parameters fit to [Emim][OAc] – pretreated *Miscanthus***
K_m cellulase	1 mM	5.51
k_{cat} cellulase	200 s^{-1}	200
K_m β-glucosidase	1.15 mM	3.88
k_{cat} β-glucosidase	558 s^{-1}	558
K_i cellulase$_{cell}$	0.01 mM	0.069
K_i cellulase$_{gluc}$	10 mM	3.89
K_i β-glucosidase$_{gluc}$	1.94 mM	0.33
R^2_{cell}		0.88
R^2_{gluc}		0.87
R^2_{tot}		1.76

Initial guesses for cellulase (Andrić et al., 2010a; Levine et al., 2010; Levine et al., 2011) and β-glucosidase (Bohlin et al., 2010) kinetic parameters from the literature.

Table 3. The kinetic constants solved for by fitting the model to the glucose and cellobiose data from the hydrolysis of [Emim][OAc] – pretreated *Miscanthus* (16.1 g/L initial glucose).

4. Conclusions

The enzymatic hydrolysis of Avicel, [Emim][OAc] – pretreated Avicel, and [Emim][OAc] - pretreated *Miscanthus* with a *T. reesei* cellulase cocktail, supplemented with β-glucosidase from *Aspergillus niger*, was studied under varying glucose concentrations. Initial glucose concentration was found to have a significant inhibitory effect on the conversion of cellulose to glucose. Cellobiose was found to accumulate during hydrolysis for all reactions with initial glucose concentrations > 5 g/L, peaking initially during the first 1.5 - 3 h of hydrolysis, and then slowly declining over the next 48 h. A constant cellobiose concentration was present that did not decline over 48 h for reactions with higher glucose concentrations, which likely further inhibit the cellulases and the conversion of cellulose, even with β-glucosidase supplementation. This effect is more pronounced with [Emim][OAc] - pretreated substrates. A competitive inhibition model was fit to the enzymatic hydrolysis data and found to fit moderately well to the cellobiose and glucose hydrolysis data. However, this model was unable to capture both the fast initial glucose production and constant cellobiose presence, highlighting the need for a more mechanistic kinetic model.

Acknowledgements

This work was funded by the Energy Biosciences Institute. We thank Mahmoud K. F. Abouelnasr for helpful discussions.

References

Andrić, P., Meyer, A.S., Jensen, P.A., Dam-Johansen, K., 2010a. Effect and Modeling of Glucose Inhibition and In Situ Glucose Removal During Enzymatic Hydrolysis of Pretreated Wheat Straw. Appl. Biochem. Biotechnol. 160, 280-297.

Andrić, P., Meyer, A.S., Jensen, P.A., Dam-Johansen, K., 2010b. Reactor design for minimizing product inhibition during enzymatic lignocellulose hydrolysis II. Quantification of inhibition and suitability of membrane reactors. Biotechnol. Adv. 28, 407-425.

Andrić, P., Meyer, A.S., Jensen, P.A., Dam-Johansen, K., 2010c. Reactor design for minimizing product inhibition during enzymatic lignocellulose hydrolysis: I. Significance and mechanism of cellobiose and glucose inhibition on cellulolytic enzymes. Biotechnol. Adv. 28, 308-324.

Bansal, P., Hall, M., Realff, M.J., Lee, J.H., Bommarius, A.S., 2009. Modeling cellulase kinetics on lignocellulosic substrates. Biotechnol. Adv. 27, 833-848.

Bio-Rad. Bio-Rad Protein Assay. LIT33 Rev C.

Bohlin, C., Olsen, S.N., Morant, M.D., Patkar, S., Borch, K., Westh, P., 2010. A comparative study of activity and apparent inhibition of fungal β-glucosidases. Biotechnol. Bioeng. 107, 943-952.

Briggs, G.E., Haldane, J.B.S., 1925. A note on the kinetics of enzyme action. Biochem. J. 19, 338-9.

Calsavara, L.P.V., De Moraes, F.F., Zanin, G.M., 1999. Modeling cellobiose hydrolysis with integrated kinetic models. Appl. Biochem. Biotechnol. 77-79, 789-806.

Chauve, M., Mathis, H., Huc, D., Casanave, D., Monot, F., Ferreira, N., 2010. Comparative kinetic analysis of two fungal β-glucosidases. Biotechnol. Biofuels 3, 1-8.

Dekker, R.F.H., 1986. Kinetic, Inhibition, and Stability Properties of a Commercial β-D-Glucosidase (Cellobiase) Preparation from Aspergillus niger and Its Suitability in the Hydrolysis of Lignocellulose. Biotechnol. Bioeng. 28, 1438-1442.

Gan, Q., Allen, S.J., Taylor, G., 2002. Design and operation of an integrated membrane reactor for enzymatic cellulose hydrolysis. Biochem. Eng. J. 12, 223-229.

Gan, Q., Allen, S.J., Taylor, G., 2003. Kinetic dynamics in heterogeneous enzymatic hydrolysis of cellulose: an overview, an experimental study and mathematical modelling. Process Biochem. 38, 1003-1018.

Ghose, T.K., 1987. Measurement of Cellulase Activities. Pure Appl. Chem. 59, 257-268.

Gruno, M., Väljamäe, P., Pettersson, G., Johansson, G., 2004. Inhibition of the Trichoderma reesei cellulases by cellobiose is strongly dependent on the nature of the substrate. Biotechnol. Bioeng. 86, 503-511.

Gusakov, A.V., Sinitsyn, A.P., 1992. A Theoretical Analysis of Cellulase Product Inhibition: Effect of Cellulase Binding Constant, Enzyme/Substrate Ratio, and β-Glucosidase Activity on the Inhibition Pattern. Biotechnol. Bioeng. 40, 663-671.

Gusakov, A.V., Sinitsyn, A.P., Klyosov, A.A., 1987. Factors Affecting the Enzymatic Hydrolysis of Cellulose in Batch and Continuous Reactors: Computer Simulation and Experiment. Biotechnol. Bioeng. XXIX, 906-910.

Gusakov, A.V., Sinitsyn, A.P., Klyosov, A.A., 1985. Kinetics of the enzymatic hydrolysis of cellulose: 1. A mathematical model for a batch reactor process. Enzyme Microb. Technol. 7, 346-352.

Holtzapple, M., Cognata, M., Shu, Y., Hendrickson, C., 1990. Inhibition of Trichoderma reesei cellulase by sugars and solvents. Biotechnol. Bioeng. 36, 275-287.

Jørgensen, H., Kristensen, J.B., Felby, C., 2007. Enzymatic conversion of lignocellulose into fermentable sugars: challenges and opportunities. Biofuels, Bioprod. Biorefin. 1, 119-134.

Kadam, K.L., Rydholm, E.C., McMillan, J.D., 2004. Development and Validation of a Kinetic Model for Enzymatic Saccharification of Lignocellulosic Biomass. Biotechnol. Prog. 20, 698-705.

Katz, M., Reese, E.T., 1968. Production of glucose by enzymatic hydrolysis of cellulose. Appl. Microbiol. 16, 419-420.

Khodaverdi, M., Jeihanipour, A., Karimi, K., Taherzadeh, M.J., 2011. Kinetic modeling of rapid enzymatic hydrolysis of crystalline cellulose after pretreatment by NMMO. J. Ind. Microbiol. Biotechnol. 39, 429-438.

Klein-Marcuschamer, D., Oleskowicz-Popiel, P., Simmons, B.A., Blanch, H.W., 2011. The challenge of enzyme cost in the production of lignocellulosic biofuels. Biotechnol. Bioeng. 109, 1083-1087.

Levine, S.E., Fox, J.M., Blanch, H.W., Clark, D.S., 2010. A mechanistic model of the enzymatic hydrolysis of cellulose. Biotechnol. Bioeng. 107, 37-51.

Levine, S.E., Fox, J.M., Clark, D.S., Blanch, H.W., 2011. A mechanistic model for rational design of optimal cellulase mixtures. Biotechnol. Bioeng. 108, 2561-2570.

Levinson, H.S., Mandels, G.R., Reese, E.T., 1951. Products of enzymatic hydrolysis of cellulose and its derivatives. Arch. Biochem. Biophys. 31, 351-365.

Michaelis, L., Menten, M.L., 1913. Die kinetik der invertinwirkung. Biochem. z 49, 333-369.

Murphy, L., Bohlin, C., Baumann, M.J., Olsen, S.N., Sørensen, T.H., Anderson, L., Borch, K., Westh, P., 2013. Product inhibition of five Hypocrea jecorina cellulases. Enzyme Microb. Technol. 52, 163-169.

Oh, K.-K., Kim, S.-W., Jeong, Y.-S., Hong, S.-I., 2000. Bioconversion of Cellulose into Ethanol by Nonisothermal Simultaneous Saccharification and Fermentation. Appl. Biochem. Biotechnol. 89, 15-30.

Reese, E.T., Gilligan, W., Norkrans, B., 1952. Effect of cellobiose on the enzymatic hydrolysis of cellulose and its derivatives. Physiol. Plant. 5, 379-390.

Selig, M., Weiss, N., Ji, Y. 2008. Enzymatic Saccharification of Lignocellulosic Biomass: Laboratory Analytical Procedure (LAP), (Ed.) National Renewable Energy Laboratory. Golden, CO, pp. 1-8.

Shill, K., Miller, K., Clark, D.S., Blanch, H.W., 2012. A model for optimizing the enzymatic hydrolysis of ionic liquid-pretreated lignocellulose. Bioresour. Technol. 126, 290-297.

Sternberg, D., Vijayakumar, P., Reese, E.T., 1977. β-Glucosidase: microbial production and effect on enzymatic hydrolysis of cellulose. Can. J. Microbiol. 23, 139-147.

Wald, S., Wilke, C.R., Blanch, H.W., 1984. Kinetics of the Enzymatic Hydrolysis of Cellulose. Biotechnol. Bioeng. XXVI, 221-230.

Watanabe, T., Sato, T., Yoshioka, S., Koshijima, T., Kuwahara, M., 1992. Purificication and properties of Aspergillus niger β-glucosidase. Eur J Biochem 209, 651-659.

Xiao, Z., Zhang, X., Gregg, D.J., 2004. Effects of sugar inhibition on cellulases and β-glucosidase during enzymatic hydrolysis of softwood substrates. Appl. Biochem. Biotechnol. 113-116, 1115-1126.

Zheng, Y., Pan, Z., Zhang, R., Jenkins, B.M., 2009. Kinetic Modeling for Enzymatic Hydrolysis of Pretreated Creeping Wild Ryegrass. Biotechnol. Bioeng. 102, 1558-1569.

Appendix

Comptetive inhibition model details:

Kinetic and inhibition equations:
(assume equilibrium for inhibition kinetics, pseudo-SS for enzyme intermediates)

$$E_c + S \underset{k_{-1}}{\overset{k_1}{\rightleftarrows}} E_cS \xrightarrow{k_{catc}} E_c + C$$

$$E_\beta + C \underset{k-2}{\overset{k_2}{\rightleftarrows}} E_\beta C \xrightarrow{k_{cat\beta}} E_\beta + 2G$$

$$E_c + C \underset{k_{-ciC}}{\overset{k_{ciC}}{\rightleftarrows}} E_cC$$

$$E_c + G \underset{k_{-ciG}}{\overset{k_{ciG}}{\rightleftarrows}} E_cG$$

$$E_\beta + G \underset{k_{-\beta iG}}{\overset{k_{\beta iG}}{\rightleftarrows}} E_\beta G$$

Equations in Excel sheet:

$$[S]_t = [S]_0 - [C]_t - \frac{1}{2}([G]_t - [G]_0)$$

$$[C]_t = [C]_{t-1} + \frac{d[C]_{t-1}}{dt}\Delta t$$

$$[G]_t = [G]_{t-1} + \frac{d[G]_{t-1}}{dt}\Delta t$$

$$\frac{d[C]}{dt} = k_{catc}[E_cS] - k_{cat\beta}[E_\beta C]$$

$$\frac{d[G]}{dt} = k_{cat\beta}[E_\beta C]$$

$$[E_cS] = \frac{[E_c][S]}{K_{mc}}$$

$$[E_c] = \frac{[E_c]_0}{1 + \frac{[S]}{K_{mc}} + \frac{[C]}{K_{cIC}} + \frac{[G]}{K_{cIG}}}$$

$$[E_\beta C] = \frac{[E_\beta][C]}{K_{m\beta}}$$

$$[E_\beta] = \frac{[E_\beta]_0}{1 + \frac{[C]}{K_{m\beta}} + \frac{[G]}{K_{\beta IG}}}$$

Constants: $[S]_0$, $[G]_0$, $[E_c]_0$, $[E_\beta]_0$
Solve for: K_{mc}, k_{catc}, $K_{m\beta}$, $k_{cat\beta}$, K_{cIC}, K_{cIG}, $K_{\beta IG}$

Derivation (Briggs and Haldane, 1925; Michaelis and Menten, 1913):

Mass and enzyme balances:

$$[S]=[S]_0-[C]-\frac{1}{2}([G]-[G]_0)$$

$$[E_c]=[E_c]_0-[E_cC]-[E_cS]-[E_cG]$$

$$[E_\beta]=[E_\beta]_0-[E_\beta C]-[E_\beta G]$$

Kinetic constants:

$$K_{mc}=\frac{k_{-1}+k_{catc}}{k_1} \quad K_{mc}=\frac{k_{-2}+k_{cat\beta}}{k_2}$$

$$K_{cIC}=\frac{k_{-ciC}}{k_{ciC}} \quad K_{cIG}=\frac{k_{-ciG}}{k_{ciG}} \quad K_{\beta IG}=\frac{k_{-\beta iG}}{k_{\beta iG}}$$

Rate equations (assume equilibrium for inhibition kinetics, pseudo-SS for enzyme intermediates) put in terms of k_{cat} and K_m:

$$\begin{aligned}\frac{d[C]}{dt}&=k_{catc}[E_cS]-k_2[E_\beta][C]+k_{-2}[E_\beta C]\\&=k_{catc}[E_cS]-k_2K_{m\beta}[E_\beta C]+k_{-2}[E_\beta C]\\&=k_{catc}[E_cS]+[E_\beta C](k_{-2}-k_2K_{m\beta})\\&=k_{catc}[E_cS]+[E_\beta C](k_{-2}-k_2(\frac{k_{-2}+k_{cat\beta}}{k_2}))\\&=k_{catc}[E_cS]-k_{cat\beta}[E_\beta C]\end{aligned}$$

$$\frac{d[G]}{dt}=k_{cat\beta}[E_\beta C]$$

Enzyme rate expressions in terms of k_{cat}, K_m:

Cellulases:

$$\frac{d[E_c]}{dt}=\frac{d[E_cS]}{dt}=\frac{d[E_cC]}{dt}=\frac{d[E_cG]}{dt}=0$$

$$\frac{d[E_cS]}{dt}=0=k_1[E_c][S]-k_{-1}[E_cS]-k_{catc}[E_cS]$$

$$[E_cS]=\frac{k_1[E_c][S]}{k_{-1}+k_{catc}}=\frac{[E_c][S]}{K_{mc}}$$

$$\frac{d[E_cC]}{dt}=0=k_{ciC}[E_c][C]-k_{-ciC}[E_cC]$$

$$[E_cC]=\frac{k_{ciC}[E_c][C]}{k_{-ciC}}=\frac{[E_c][C]}{K_{cIC}}$$

$$\frac{d[E_cG]}{dt}=0=k_{ciG}[E_c][G]-k_{-ciG}[E_cG]$$

$$[E_cG]=\frac{k_{ciG}[E_c][G]}{k_{-ciG}}=\frac{[E_c][G]}{K_{cIG}}$$

$$[E_c]=[E_c]_0-[E_cS]-[E_cC]-[E_cG]$$

$$[E_c]=[E_c]_0-\frac{[E_c][S]}{K_{mc}}-\frac{[E_c][C]}{K_{cIC}}-\frac{[E_c][G]}{K_{cIG}}$$

$$[E_c]=\frac{[E_c]_0}{1+\frac{[S]}{K_{mc}}+\frac{[C]}{K_{cIC}}+\frac{[G]}{K_{cIG}}}$$

β-glucosidase:

$$\frac{d[E_\beta]}{dt}=\frac{d[E_\beta C]}{dt}=\frac{d[E_\beta G]}{dt}=0$$

$$\frac{d[E_\beta C]}{dt}=0=k_2[E_\beta][C]-k_{-2}[E_\beta C]-k_{cat\beta}[E_\beta C]$$

$$[E_\beta C]=\frac{k_2[E_\beta][C]}{k_{-2}+k_{cat\beta}}=\frac{[E_\beta][C]}{K_{m\beta}}$$

$$\frac{d[E_\beta G]}{dt}=0=k_{\beta iG}[E_\beta][G]-k_{-\beta iG}[E_\beta G]$$

$$[E_\beta G]=\frac{k_{\beta iG}[E_\beta][G]}{k_{-\beta iG}}=\frac{[E_\beta][G]}{K_{\beta IG}}$$

$$[E_\beta]=[E_\beta]_0-\frac{[E_\beta][C]}{K_{m\beta}}-\frac{[E_\beta][G]}{K_{\beta IG}}$$

$$[E_\beta]=\frac{[E_\beta]_0}{1+\frac{[C]}{K_{m\beta}}+\frac{[G]}{K_{\beta IG}}}$$

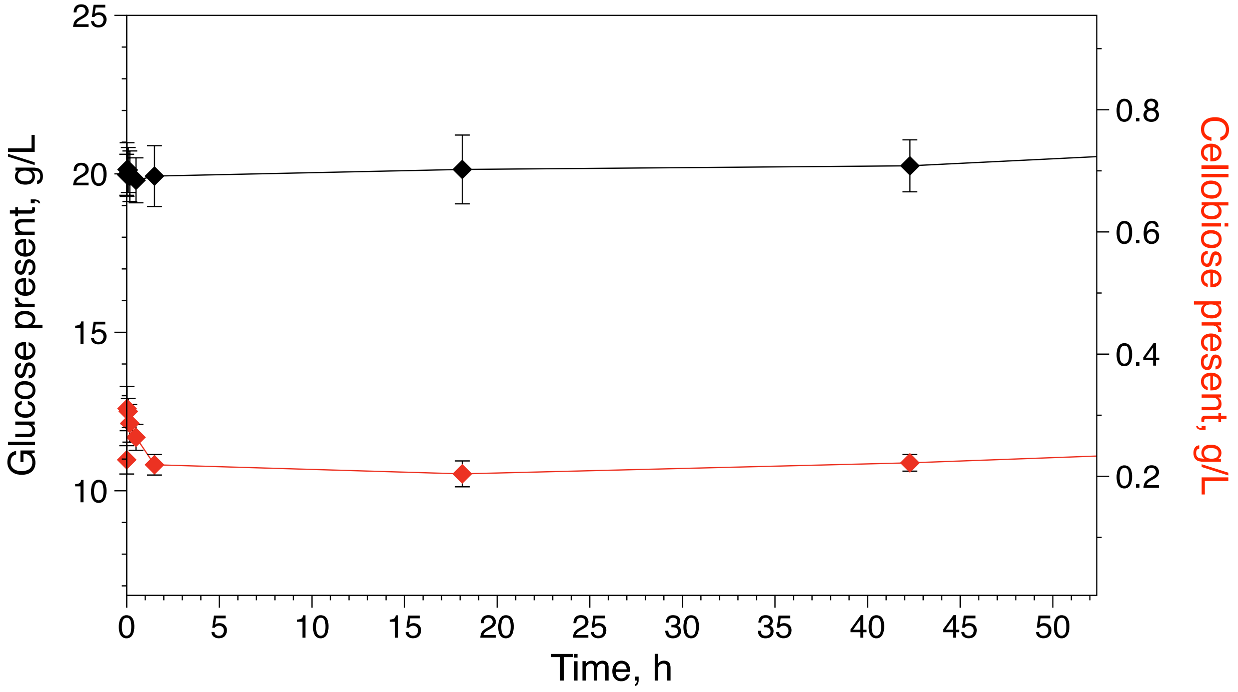

Figure A1. The glucose (black) and cellobiose (red) concentration curves present for a reaction containing only glucose, cellobiose, and β-glucosidase. Error bars represent one standard deviation.

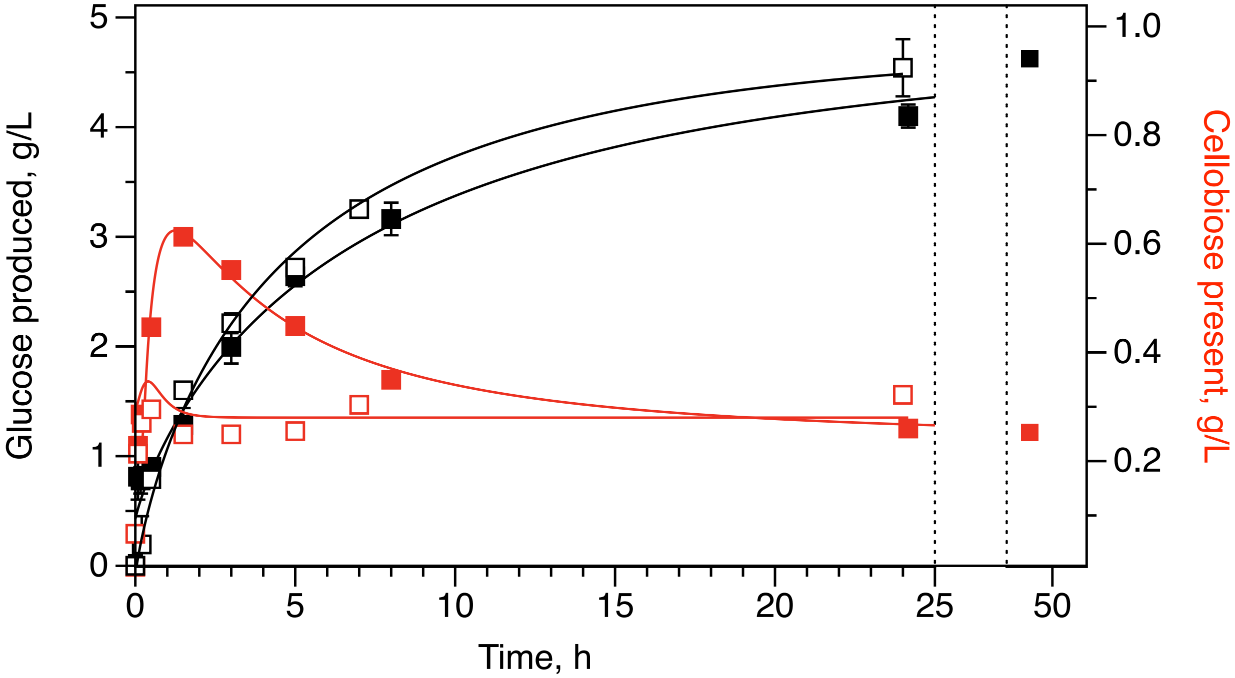

Figure A2. The enzymatic conversion of Avicel to cellobiose (red) and glucose (black) with varying initial β-glucosidase concentrations (■ - 16.2 g/L initial glucose, □ – 17.5 g/L initial glucose, 10x Novo188). Error bars represent one standard deviation.

(a)

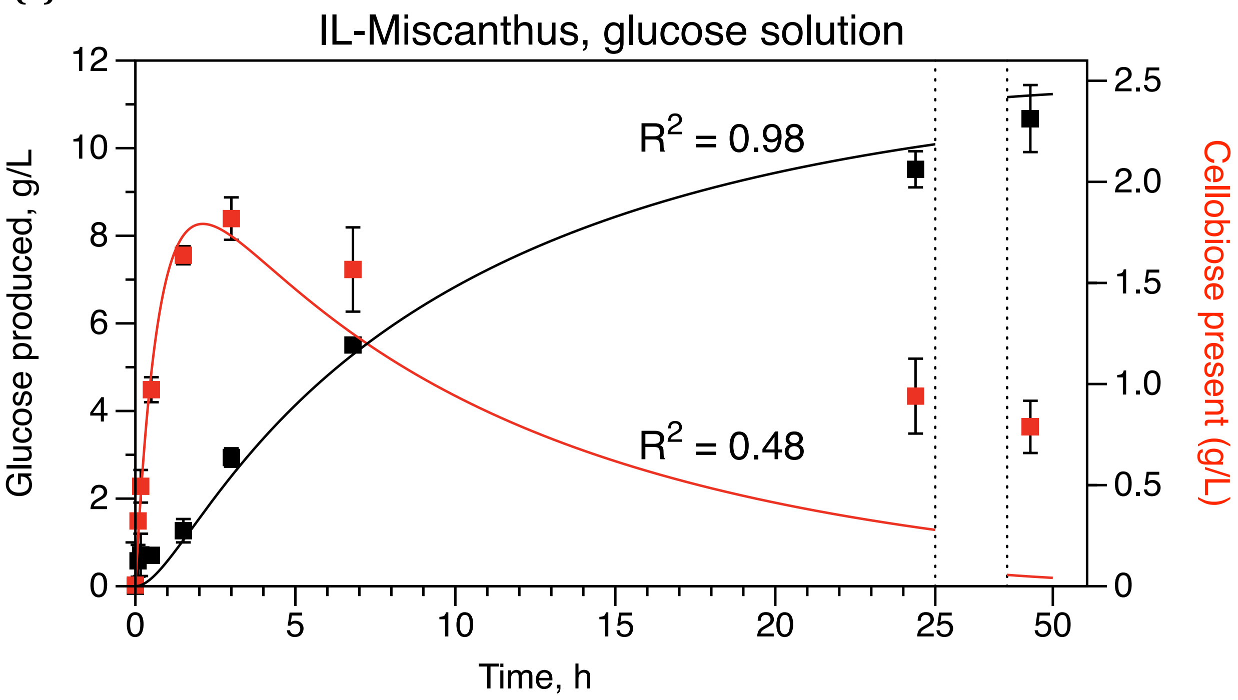

(b)

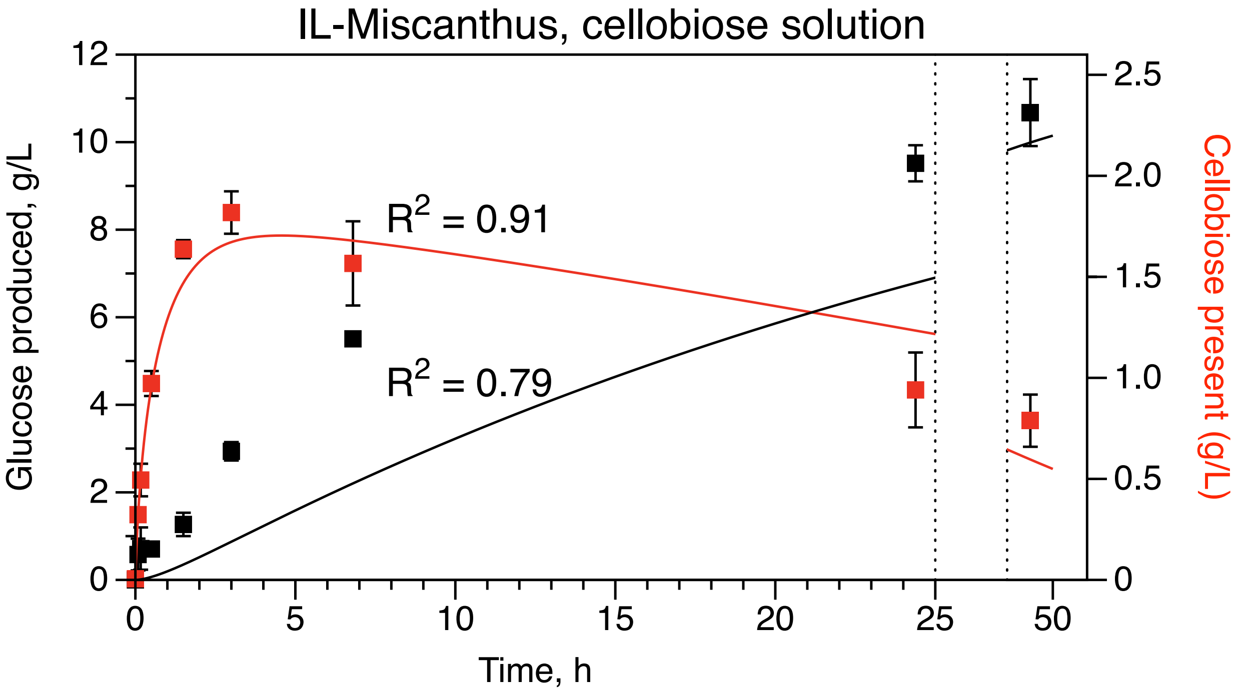

Figure A3. The enzymatic conversion of [Emim][OAc]-pretreated *Miscanthus* to cellobiose (red) and glucose (black) with 16.1 g/L initial glucose concentration. The lines represent the model's predicted cellobiose and glucose concentrations. The model was fit to either glucose (a), or cellobiose (b).